Received: 19 February 2024 | Revised: 27 March 2024 | Accepted: 28 March 2024

DOI: 10.1002/psc.3606

REVIEW

Journal of PeptideScience WILEY

# Peptides and metal ions: A successful marriage for developing artificial metalloproteins

Linda Leone[1] | Maria De Fenza[1] | Alessandra Esposito[1] | Ornella Maglio[1,2] | Flavia Nastri[1] | Angela Lombardi[1]

[1]Department of Chemical Sciences, University of Naples Federico II, Naples, Italy

[2]Institute of Biostructures and Bioimaging, National Research Council, Naples, Italy

**Correspondence**
Angela Lombardi and Flavia Nastri, Department of Chemical Sciences, University of Naples Federico II, Via Cintia, 80126, Naples, Italy.
Email: alombard@unina.it and flavia.nastri@unina.it

**Funding information**
Italian Ministry of University and Research (MUR) "Dipartimenti di Eccellenza 2023-2027" program, arCHIMede project, Grant/Award Number: E63C22003710006; Programma Operativo Nazionale Ricerca e Innovazione (PON R&I), Grant/Award Numbers: E65F21003010003, E65F21003750003; European Research Council (ERC), UGOV 000005_HORIZON2020_ERC_2018_ BioDisOrder Project, Grant/Award Number: E64I19002960006; Italian Ministry of University and Research (MUR), PRIN2020 program, Project SEAWAVE 2020BKK3W9, Grant/Award Number: E69J22001140005; CRUI-CARE WILEY Agreement with University of Naples Federico II

The mutual relationship between peptides and metal ions enables metalloproteins to have crucial roles in biological systems, including structural, sensing, electron transport, and catalytic functions. The effort to reproduce or/and enhance these roles, or even to create unprecedented functions, is the focus of protein design, the first step toward the comprehension of the complex machinery of nature. Nowadays, protein design allows the building of sophisticated scaffolds, with novel functions and exceptional stability. Recent progress in metalloprotein design has led to the building of peptides/proteins capable of orchestrating the desired functions of different metal cofactors. The structural diversity of peptides allows proper selection of first- and second-shell ligands, as well as long-range electrostatic and hydrophobic interactions, which represent precious tools for tuning metal properties. The scope of this review is to discuss the construction of metal sites in de novo designed and miniaturized scaffolds. Selected examples of mono-, di-, and multi-nuclear binding sites, from the last 20 years will be described in an effort to highlight key artificial models of catalytic or electron-transfer metalloproteins. The authors' goal is to make readers feel like guests at the marriage between peptides and metal ions while offering sources of inspiration for future architects of innovative, artificial metalloproteins.

**KEYWORDS**
artificial enzymes, catalysis, de novo design, electron transfer, metal ions, metalloprotein models, peptides

**Abbreviations:** 2SCC, two-stranded coiled coil; 3HB, three-helix bundle; 3SCC, three-stranded coiled coil; 4-AP, 4-aminophenol; 4-BQM, 4-benzoquinone monoamine; 4SCC, four-stranded coiled coil; ADT, 2-aza-propane-(1,3)-dithiolate; ArCuP, artificial copper protein; ArH, artificial hydrogenase; AurF, *p*-aminobenzoate N-oxygenase; BMMs, bacterial multicomponent monooxygenases; CA, carbonic anhydrase; CaHydA, *Clostridium acetobutylicum* [FeFe]-hydrogenase; CCIS, coiled coil iron-sulfur protein; CcO, cytochrome c oxidase; CD, circular dichrosim; CED, computational enzyme design; CH, chelate; ChC, chelate core; *Cp*, *Clostridium pasteurianum*; CR, core; Csp1, copper storage protein; CuNiR, copper nitrite reductase; DA, Diels-Alderase; DF, due ferri; DMF, dimethylformamide; DMP, dimethoxyphenol; DR, due rame; DSD, domain-swapped dimers; DTBC, 2,3-di-tert-butyl-cathecol; DTBQ, 2,3-di-tert-butyl-quinone; EPR, electron paramagnetic resonance; ET, electron transfer; FDA, food and drug administration; FdM, ferredoxin maquette; FeS, iron-sulfur; GR, grand family of peptides; HER, hydrogen evolution reaction; LMPO, lytic polysaccharide monooxygenases; MC, mimochrome; MCO, multicopper oxidases; METP, miniaturized electron transfer protein; MID, metal interface design; MMOs, methane monooxygenases; MPs, metalloproteases; MSD, multi state design; NBP, nickel binding protein; NHE, normal hydrogen electrode; NMR, nuclear magnetic resonance; $N_2OR$, nitrous oxide reductase; NiSOD, nickel superoxide dismutase; NPAA, non-proteinogenic amino acids; PAC, perturbed angular correlation; *p*NPA, para-nitrophenylacetate; *p*NPP, para-nitrophenylphosphate; PDB, protein data bank; PPO, polyphenol oxidase; PS, porphyrin-binding sequence; PSI/II, photosystem I/II; RM1, rubredoxin mimic 1; Rds, rubredoxins; Sec, selenocysteine; *SHE*, standard hydrogen electrode; Sp1f2, specificity protein 1 finger 2; $SQ^{\cdot-}$, semiquinone radical; TEOA, triethanolamine; T1Cu, type 1 copper; T2Cu, type 2 copper; T3Cu, type 3 copper; TEA, triethylamine; TON, turnover number; TOMO, toluene monooxygenase; UFsc, uno ferro single-chain; XAS, X-ray absorption spectroscopy; ZnP, Zn-porphyrin.

## 1 | INTRODUCTION

The tremendous progress in design strategies and computational tools,[1–5] the infinite array of sequences that can be produced (either by chemical synthesis[6–8] or recombinant methods[9,10]) and the deep knowledge of the principles governing peptide folding and stability,[11–13] currently allow obtaining peptide-based molecules with customizable behaviors. While peptides share the same amino acid building-blocks as proteins, they can be easily tailored with a range of modifications, which include the incorporation of non-proteogenic amino acids (NPAAs), but also backbone (methylation, acetylation)[14,15] and sidechain (glycosylation, phosphorylation)[16–18] functionalization. Such chemical modifications may have the potential to dramatically alter the conformation of a peptide, which represents a crucial aspect in developing functional molecules. All these valuable aspects make designed peptides amenable for an extensive range of applications, such as in biomedicine,[19] as therapeutic agents[20] or molecular imaging probes,[21] or, more recently as innovative materials.[22,23] Peptide-based nanospheres, nanotubes, fibers, wires, and monolayers have been prepared and used as electro−/photoactive materials and smart platforms for drug delivery and tissue engineering.[24] Thanks to the possibility of generating such a variety of molecular architectures, starting from simple basic motifs, the application of peptide-based structures spreads also in catalysis.[25–27] Taking inspiration from Nature, peptides can be used to mimic enzyme active sites because they can be designed as precise replicas of protein fragments. In addition, catalytic functions can be implanted into peptide scaffolds with structures completely different and unrelated to natural systems. In summary, peptide-based structures represent a blank canvas on which researchers may 'paint' diverse functionalities. This aspect is especially reliable for developing artificial metalloproteins.[28–30]

Most proteins involved in essential biochemical processes rely on metal cofactors to accomplish their functions. Despite a limited number of metal ions are found in metalloenzymes, these can display countless kinds of activities.[31] This incredible diversity arises from the synergistic cooperation between metal ions and protein scaffolds, which modulate their properties each other through specific interactions. Metalloproteins can be considered as special coordination compounds, with the protein scaffold representing a sophisticated macromolecular ligand.[32] In this respect, the protein matrix directs the properties of the metal ion by dictating the nature and the arrangement of ligands in the first coordination shell.[33] An additional level of control is provided by second shell-interaction, as well as long-range electrostatic and hydrophobic interactions within the surrounding protein environment. These factors strongly influence the ligand field strength and, consequently, the redox properties of the metal cofactor, thus enabling similar sites to perform divergent reactivities. Unraveling the intricate mechanisms at the basis of metalloprotein functions has been the subject of intense research for several decades. A relevant approach for this purpose consists in lowering the complexity found in natural systems and reproducing metalloproteins activity into model compounds.[34–39] In particular, the integration between peptides and metal ions may afford limitless combinations of metal binding sites, which may serve different functions, ranging from structural role to electron transfer and catalysis.[40]

The most challenging aspect in designing metal-binding sites into peptide-based structures is the construction of any desired catalytic functions, either natural or "unknown to Nature".[41–45] To achieve this difficult task, multiple factors should be considered. First, catalysis by metalloenzymes is usually associated with metal ion redox activity, thus the ligand platform should be able to fulfill the coordination requirements of a metal in different oxidation states.[46] Further, many enzymatic reactions are assisted by the amino acid residues in the proximity of the metal site, which act as proton shuttles or facilitate substrate activation through direct interactions. Finally, the three-dimensional protein structure discriminates among different substrates and ensures their precise positioning within the active site, giving rise to the exceptional selectivity of metalloenzymes. To achieve such a level of control, the ligand architecture requires an appropriate degree of complexity, which is somehow difficult to reproduce in small-molecule coordination compounds.[47] In this respect, peptides represent a balanced compromise between the simplicity of small-molecules and the complexity of protein structures. Indeed, they possess adequate size and chemical diversity for satisfying the structural requirements of a functional metal center. By joining the power of different and complementary strategies, peptide scaffolds can be shaped and optimized to accommodate metal binding sites and tune their reactivity.[48]

Currently, a variety of functions are being implanted into peptide/protein scaffolds, thus producing artificial metalloproteins and metalloenzymes.[26] We are aware that it is impossible to exhaustively cover the huge amount of work in the field. For this reason, the elegant approaches based on metalloprotein repurposing and other fascinating examples, such as the insertion of synthetic catalytically competent metal cofactors into naturally occurring proteins, are not covered here, and readers can refer to other excellent reviews on these topics.[49–58]

In this review, we will illustrate the efforts made in reproducing the activities of metalloproteins into entirely designed peptide-based systems. We will mainly focus on artificial metalloenzymes obtained through miniaturization and de novo peptide design. The miniaturization approach seeks to identify in the inspiring natural metalloprotein the least number of interactions necessary to maintain the structural and functional integrity of the metal center.[59] These are then reproduced into the smallest possible self-sufficient peptide fragment. The de novo design aims at generating "from scratch" a desired structure (and function) with a peptide sequence unrelated to naturally occurring proteins.[60,61] The metal binding site is then engineered into the de novo peptide scaffold, introducing and stabilizing the ligands through properly designed interactions.

Nowadays, several structural motifs can be designed with the highest degree of confidence and offer the benefit of withstanding significant mutations.[62] This is the case of α-helical bundles,[63] which have been widely used as templates for inserting a variety of metal centers. It is relevant to note that metal binding sites have different levels of "designability", as some sites are more easily reproduced than others. For instance, in heme centers the metal ion is tightly

chelated by the porphyrin ligand, which greatly stabilizes the complex.[64] The peptide scaffold contributes to the first coordination shell by supplying solely the axial ligand/s and exerts a fine modulation by shaping the surrounding environment. Conversely, it is more difficult to reproduce clusters, which feature bridging ligands and multiple metal ions, where a subtle equilibrium between stability and flexibility must be achieved.[65] Therefore, we will not examine in this review the considerable amount of work that has been devoted to replicating the incredible catalytic promiscuity of heme-enzymes by using peptide scaffolds. The reader can refer to recent literature on the subject.[66–81]

Starting from the analysis of metal centers found in natural proteins, we will illustrate representative examples mainly acting as models of catalytic or electron transfer metalloproteins. These will be organized according to the different coordination environments of the metal ions that have been implanted into peptide scaffolds. We will describe metal binding sites with increasing level of complexity, starting from mononuclear to dinuclear, and finally to multinuclear metal sites.

## 2 | PEPTIDE SCAFFOLDS HOUSING MONONUCLEAR METAL BINDING SITES

Over the past few decades, an extensive library of engineered peptide scaffolds housing mononuclear binding sites was collected.[49] A wide range of transition metals were incorporated in fine-tuned chemical environments, providing functional metalloproteins with diverse activities. In the next two paragraphs, we will highlight the plethora of functions that have been incorporated in different scaffolds, comprising helical bundles, zinc finger, and β-hairpin motifs, de novo amyloid fibrils. The role of the metal ion in directing different activities will be underlined. We categorize the challenge of developing artificial peptides/proteins that incorporate mononuclear sites into catalytic and electron-transfer sites.

### 2.1 | Artificial metalloproteins housing mononuclear catalytic sites

The seminal work of Pecoraro and his research group in constructing mononuclear metal-binding sites into designed peptide-based scaffolds represents an impressive contribution to this field. Indeed, they reached important milestones in the de novo design of artificial metalloproteins by introducing mononuclear catalytic sites in designed three-stranded coiled coils (3SCC), namely TRI and GRAND (GR) peptides. Mutations in the first and second coordination spheres of selected metals (Table 1) led them to reproduce natural enzymatic activities in an artificial scaffold.

The hydrolytic activity of carbonic anhydrases (CAs) was explored initially. Natural CAs catalyze the physiological reversible hydration of $CO_2$ with TON till to $10^6$.[92] However, CAs are also known to catalyze many other reactions, such as the hydrolysis of several additional substrates.[93] All 16 recognized isoforms of CAs possess a structure primarily composed of β-strands.[94] This structure specifically comprises a set of 10 β-strands forming a twisted β-pattern, surrounded by six α-helices on the protein surface. The active site resides within a cavity close to the protein core, wherein Zn(II) binds to three His residues and a solvent molecule, arranged in a tetrahedral geometry.[95] The artificial scaffold used by Pecoraro to model the active site of CA is based on the TRI-family peptide sequence (Table 1), in which the helical structure is designed based on a heptad repeat approach. Notably, the CA binding site was reproduced in a peptide fold completely unrelated to the natural CA fold (α-helical versus β-sheets).[90,96] Furthermore, the CA model ($[Hg(II)]_5[Zn(II)(H_2O/OH^-)]_N$(TRIL9CL23H)$_3^+$) they designed represented the first example of a peptide-based artificial metalloenzyme housing two metal-binding sites with distinct functions (catalytic and structural). The catalytic function was accomplished by a pseudo tetrahedral Zn(II)$His_3$ site (as in natural CA), while the structural role was provided by a trigonal Hg(II)$Cys_3$ site. The resulting metalloenzyme was proven to be a highly efficient CA-mimic. Indeed, it catalyzed the hydrolysis of *p*-nitrophenyl acetate (*p*NPA) as a model substrate with a catalytic efficiency that was only ~100-fold lower with respect to CA-II, the fastest α-CA isozyme. Remarkable activity in the hydration of $CO_2$ was observed, with a catalytic efficiency that is within ~500-fold that of CA-II. Notably, this de novo designed metalloprotein behaves as the best CA mimic reported to date, displaying a ~ 500-fold higher hydrolytic activity and an over 70-fold better $CO_2$ hydration activity with respect to any previously reported small-molecule synthetic model.[97,98] This work showcases the power of de novo peptide design in the successful reconstruction of the essential components required for catalytic activity, within a peptide fold, entirely distinct from that found in the natural enzyme.

Nonetheless, the symmetric nature of this peptide scaffold showed as a limitation the failure in replicating precise interactions, such as an extended H-bond network, found in the natural enzymes, and important for function. In an attempt to overcome the symmetry limitations, the same authors used a single-stranded antiparallel three-helix bundle, named $\alpha_3$D, previously developed by DeGrado and co-workers[99] to construct a CA model. Three Leu residues in the C-terminal region of $\alpha_3$D were substituted with three His, leading to $\alpha_3$DH3.[100] The latter model was able to bind Zn(II), and the resulting complex was found to catalyze the $CO_2$ hydration reaction with a catalytic efficiency 14-fold higher compared to the top-performing small molecule models,[97,98] but it fell slightly lower in efficiency when compared to TRI-based compounds.[90]

The development of de novo scaffolds, housing redox-active metal centers, is even more challenging.

In this case, the coordination environment should be able to accommodate the metal ion in different oxidation states. Pecoraro and coworkers accomplished this goal by implanting the catalytic site of the copper nitrite reductases (CuNiRs) within the above-described TRI scaffold.[91,101] Natural CuNiRs are homotrimeric metalloenzymes containing two copper binding sites: a type 1 copper center (T1Cu) and a type 2 copper center (T2Cu).[102] T1Cu centers are characterized by a conserved ligand composition, comprising two histidines and a cysteine residue arranged in a trigonal planar geometry. The presence and the nature of axial ligands are usually variable and, in many cases,

**TABLE 1** Peptide scaffolds within TRI family housing mononuclear binding sites with structural or catalytic role.

| TRI peptide mutation | Metal | Binding site | Coordination geometry | Ref. |
|---|---|---|---|---|
| *De novo designed peptide scaffolds binding heavy metals* | | | | |
| TRIL16C | Hg(II) | S2/S3 | Linear[(a)]/Trigonal planar[(b)] | 82 |
| | Cd(II) | S3/S3O | Trigonal planar (35%)/distorted pseudo-tetrahedral (65%)[(c)] | 83 |
| | Pb(II) | S3 | Trigonal pyramidal | 84 |
| | Bi(III) | S3 | Trigonal pyramidal | 84 |
| TRIL12C | Cd(II) | S3/S3O | Trigonal planar (60%)/distorted pseudo-tetrahedral (40%)[(c)] | 83 |
| | Pb(II) | S3 | Trigonal pyramidal | 84 |
| | Bi(III) | S3 | Trigonal pyramidal | 84 |
| TRIL9A/L16C | Cd(II) | S3/S3O | Trigonal planar (90%) /distorted pseudo-tetrahedral (10%)[(c)] | 85 |
| TRIL12A/L16C | Cd(II) | S3O | Distorted pseudo-tetrahedral | 85 |
| TRIL12$L_D$/L16C [(d)] | Cd(II) | S3 | Trigonal planar | 86 |
| TRIL16Pen [(e)] | Cd(II) | S3 | Trigonal planar | 87 |
| GRL16CL30H | Pb(II) | S3 | Trigonal pyramidal | 88 |
| TRIL12AL16 | Zn(II) | S3O | Distorted pseudo-tetrahedral | 88 |
| TRIL9C | As(III) | S3 | Trigonal pyramidal | 89 |
| *De novo designed peptide scaffolds for catalysis* | | | | |
| TRIL9CL23H | Hg(II) | S3 | Trigonal planar | 90 |
| | Zn(II) | N3O | Distorted pseudo-tetrahedral | 90 |
| TRIL23H | Cu(I) | N3O | Distorted trigonal-planar | 91 |
| | Cu(II) | N3O2 | Pentacoordinate | 91 |

TRI: Ac-G-$(LKALEEK)_4$-G-$NH_2$; GRAND (GR): Ac-G-$(LKALEEK)_5$-G-$NH_2$.
[(a)]Prevalent at low peptide/Hg(II) ratio.
[(b)]prevalent at high peptide/Hg(II) ratio.
[(c)]a mixture of coordination environments was observed. The relative % was determined by $^{113}$Cd nuclear magnetic resonance (NMR) and $^{(111m)}$Cd perturbed angular correlation (PAC) spectroscopy.
[(d)]$L_D$: D-Leucine; [(e)]Pen: penicillamine.

one position is occupied by a methionine residue.[103–106] Conversely, T2Cu centers typically contain three histidine residues and one or two solvent molecules.[103–106] While the former usually function as electron transfer units in biological processes, the latter display catalytic activity toward small-molecule substrates, such as dioxygen.[103–106] In CuNiR, the T2Cu site ($[Cu(I)(His)_3(OH_2)]$) catalyzes the reduction of nitrite to nitric oxide ($NO_2^- + e^- + 2H^+ = NO + H_2O$), a key step in the nitrogen cycle, occurring in a wide range of denitrifying bacteria and fungi, while the T1Cu site provides the electron necessary for the reduction of nitrite.[107] Since the T2Cu site of CuNiR and the Zn(II) binding site of CA share a similar $His_3$ coordination environment, swapping zinc with copper was chosen as a strategy for switching the reactivity of TRI artificial metalloproteins from hydrolase to nitrite reductase. The heavy metal structural site of the CA model was omitted, and a more simplified peptide scaffold, TRIL23H, was used to develop a CuNiR mimic. The spectroscopic analysis supported a five-coordinate Cu(II) structure with three quasi-in-plane imidazoles and one or two water molecules, while the reduced Cu(I) state showed a trigonal planar geometry.[91] The designed molecule was able to generate nitric oxide from nitrite using ascorbate as a sacrificial electron donor. Although the activity was approximatively 6 orders of magnitude below that of native CuNiR, the artificial copper site represents the first example of a functional $Cu(His)_3$ site, stable in aqueous solution and capable of multiple turnovers, with unvarying efficiency up to 3.7 h. To further enhance the activity of this CuNiR model, additional design efforts were directed toward introducing mutations in the second coordination shell of the copper ion.[108] The re-design rounds allowed an increase in the activity up to 75-fold compared to previously reported systems.[91,101] To better control the interactions in the second coordination shell, the CuNiR binding site was also engineered in the frame of an anti-parallel three-helix bundle based on the $\alpha_3$D scaffold, as described for the CA model. In this case, a lengthened version of $\alpha_3$D, namely Grand $\alpha_3$D[99] was selected for incorporating the T2Cu center, with the aim of further improving the stabilization of the metal site by packing interactions. This approach was successful since the resulting CuNiR model displayed an 18-fold enhanced catalytic efficiency compared to the analogue based on the parallel TRI scaffold.[109]

In the pursue of finding new strategies for modulating the packing interactions around the metal binding sites, the same group analyzed the impact of introducing a three-residue discontinuity, known as stammer, in the above-described 3SCC metalloproteins.[110] Stammer insertion was intended to locally alter the twist of the helix, thus exerting a destabilizing effect on the helical bundle. To balance this effect, the stammer was inserted in a larger 3SCC scaffold, belonging to the Grand family of peptides (GR), which includes an additional

heptad repeat compared to the TRI scaffold.[111] Unexpectedly, the stammer insertion into the newly designed scaffold, $GRW_{27sta\text{-}mAEL}$L33H, had divergent effects on CuNiR activity and zinc-catalyzed *p*NPA hydrolysis. Indeed, the copper complex showed significantly enhanced NiR activity, while the hydrolytic activity of the zinc complex was nearly completely ablated, close to background levels. This peculiar behavior was attributed to secondary coordination shell effects, caused by stammer inclusion above the metal binding site. X-ray absorption spectroscopic (XAS) data suggested that both metals are bound in typical coordination geometries. The reduced steric packing above the copper upon stammer insertion allows the Cu(I) ion to adopt a more linear geometry, with the formation of a more open complex. This in turn would favor the access of the small nitrite substrate, leading to an enhanced catalytic activity, as previously observed for the parent TRIW-H mutants.[108] Conversely, the Zn(II) pseudo tetrahedral geometry appears to be retained, and the helices twisting caused by the stammer incorporation may disfavor an intermediate of higher coordination number, and/or block the access of the sterically bulkier *p*NPA molecule to the Zn(II) site. In summary, a simple modification of the 3SCC scaffold may influence the first and second coordination shell properties and improve or reduce catalytic activities.

Toward the same goal of controlling the catalytic potential of the zinc ion through designed peptides, other research groups have developed de novo designed artificial hydrolases.

In this regard, MID1 (metal interface design), a homodimeric peptide, was developed by Kuhlman's group.[112] MID1 is characterized by a 46-residues helix-turn-helix motif, capable of self-assembling in the presence of zinc ions (Figure 1A). The designed model featured two zinc-binding sites, each consisting of four tetrahedrally arranged histidines. Each peptide monomer provided two His residues to each metal binding site. The crystal structure of MID1 surprisingly revealed two $ZnHis_3$ sites at the interface between monomers, with the fourth ligand position occupied by a tartrate molecule derived from the crystallization buffer, giving rise to a $(His)_3O$ coordination environment. Zn(II)-MID1 promoted the hydrolysis of carboxyester (*p*NPA) and phosphoester (*p*-nitrophenyl phosphate, *p*NPP) model substrates, catalyzing the breakdown of *p*NPA with a pH-independent rate acceleration of $10^5$ compared to background reaction, and a $k_{cat}/K_m$ value of 630 $M^{-1}$ $s^{-1}$. The same group, in collaboration with Hilvert's group, converted MID1 in its corresponding single-chain globular version (MID1sc),[113] with the aim of constructing an asymmetric protein environment around the metal site, resembling natural metalloenzymes. They connected the adjacent N- and C- termini of the monomer units by Gly-Ser-Gly linker and allowed the coordination of a single zinc ion, by replacing the metal-binding residues of the zinc site farthest from the linker, with non-coordinating amino acids. The reactivity of the asymmetric prototype MID1sc was evaluated toward the hydrolysis of a chiral ester-containing fluorogenic substrate. Notably, this approach succeeded in introducing enantioselectivity into the MID1 scaffold, since the (*R*)-configured substrate enantiomer was preferentially cleaved. However, MID1sc displayed lowered catalytic efficiency ($k_{cat}$ = 0.011 ± 0.001 $s^{-1}$ and $k_{cat}/K_m$ = 18 ± 2 $M^{-1}$ $s^{-1}$) compared to the former homodimeric analogue. Therefore, the authors optimized its catalytic activity through various rounds of mutagenesis, obtaining a model, named MID1sc10, which showed functional properties comparable to those of natural enzymes.[113] MID1sc10 hydrolyzed *p*NPA with a $k_{cat}$ value of 1.64 $s^{-1}$, which is 10,000-fold higher than the parent MID1sc. This remarkable catalytic activity was also accompanied by a 990-fold kinetic preference for the hydrolysis of the (*S*)-configured chiral phosphoester (Figure 1B).

In addition to hydrolytic activity, Zn(II)-mediated Lewis acid catalysis is widely used to promote other synthetically relevant reactions. This has inspired Hilvert and coworkers to widen the scope of

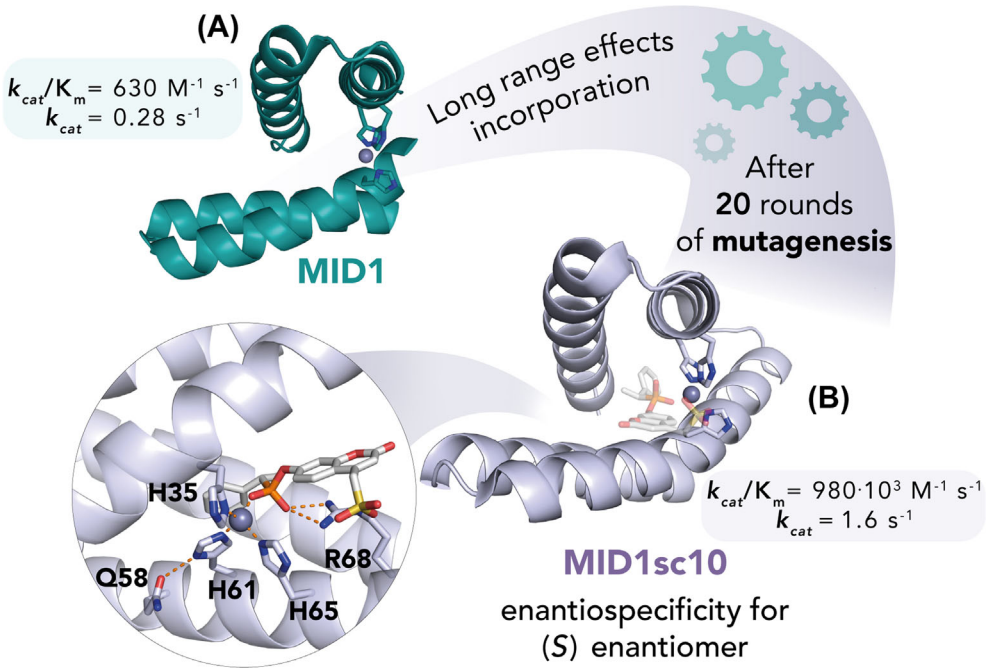


**FIGURE 1** De novo design of (A) MID1 homodimeric peptide[112] and (B) MID1sc10[113] (PDB IDs: 3V1C and 5OD1, respectively). The zinc-binding site of MID1sc10 containing the chiral substrate is highlighted in the circle. The His residues and the substrate are depicted as sticks, and the Zn(II) ion as a grey sphere. $Arg^{68}$ and $Gln^{58}$ are highlighted because they form relevant hydrogen bonds to phosphate.

reactivities accessible by MID1sc proteins, including abiological transformations. Toward this goal, the MID1sc scaffold was engineered to catalyze enantioselective Diels-Alder reactions.[114] First, a few punctual mutations were introduced to optimize the substrate binding pocket to accommodate model Diels-Alder substrates (azachalcone and 3-vinylindole). The resulting protein (DA0) displayed modest activity, but several cycles of laboratory evolution allowed for an impressive enhancement of its catalytic performances. The best-performing artificial Diels-Alderase (DA7) surpasses all the previously reported artificial metalloenzymes based on the engineering of natural protein scaffolds, performing at least $10^4$ turnovers.

De novo hydrolytic mononuclear metalloenzymes were also obtained by taking inspiration from natural zinc finger proteins, where the metal center has a structural role and lacks any catalytic activity.[115] A distinctive feature of a catalytic metal site is the presence of one or more coordination vacancies for binding and activating substrates during the catalytic cycle. Thus, converting a saturated zinc finger site into a catalytic one requires a careful redesign of the ligands in the first coordination sphere. In this context, Durani and his team de novo designed a zinc-binding site inspired by a natural zinc finger protein and repurposed the structural metal site toward hydrolytic activity (Figure 2).[116,117] The first step was the design of a 21-residue peptide adopting the αββ fold, typical of zinc finger proteins. Then, the $Cys_2His_2$ zinc finger binding site was converted into the $His_3$ zinc-binding site of CA. The zinc coordination was successfully accomplished, but the resulting complex was not able to perform *p*NPA hydrolysis. In the next step, the sequence and stereochemistry (unnatural amino acids were introduced) of such peptides were optimized, and the resulting models exhibited catalytic activity in their Zn(II) complexes. Remarkably, *p*NPA was hydrolyzed with an observed efficiency only 1,000-fold lower than that of native carbonic anhydrase (CA) (Figure 2).

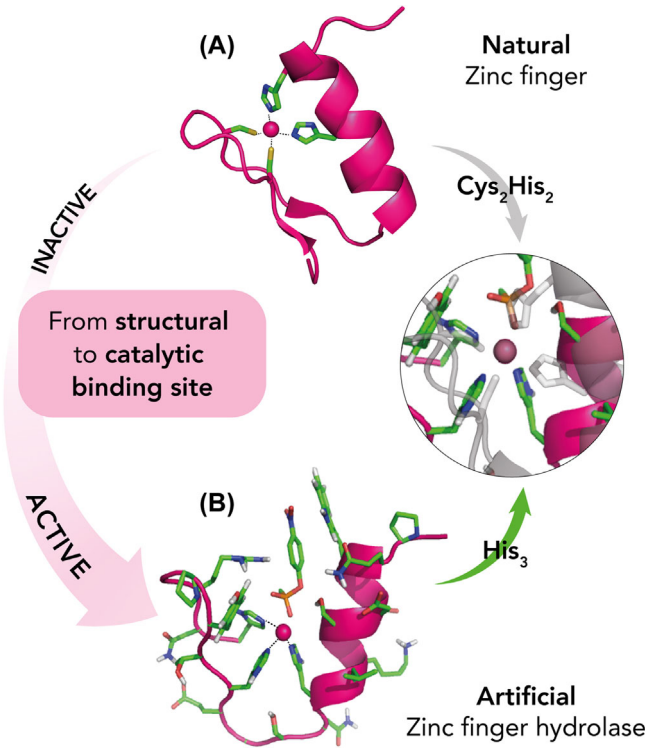


**FIGURE 2** From a natural structural binding site (A) ($His_2Cys_2$; PDB ID: 1JK2) to a hydrolytic metal-binding site (B) ($His_3$; adapted with permission from reference.[116] *Copyright: © 2014 Srivastava, Durani*). The artificial binding site (B) contains the substrate *p*NPA (*p*-nitrophenyl acetate). The residues and *p*NPA are depicted as sticks, and the Zn(II) ions as magenta spheres. The overlap of the two binding sites is highlighted within the circle.

Similarly to Durani and coworkers, Iranzo and her group developed artificial hydrolases drawing inspiration from zinc finger proteins. Toward this goal, they employed computational enzyme design (CED) approaches. Through a combination of multi-state design (MSD) and molecular dynamics simulations, they designed two peptide scaffolds able to bind a Zn(II) metal ion, and emulate the hydrolytic activity of zinc metalloproteases (MPs).[118] The first peptide, named RD01, was derived from the zinc-finger metallopeptide Sp1f2 (the finger 2 of the Sp1 transcription factor), while the second one, named RD02, was de novo designed based on the structure of villin headpiece C-terminal subdomain, HP35. Both metallopeptides adopted an α-helical conformation upon Zn(II) binding and their hydrolytic activity was tested using *p*NPA as substrate. Both RD01 and RD02 behaved as more robust catalysts compared to their natural counterpart, exhibiting TON values higher than HP35 at pH 7.5.

While all the examples above described involve the incorporation of hydrolytic zinc sites into predominantly α-helical peptide scaffolds, DeGrado, Korendovich, and coworkers implemented a catalytic zinc site within amyloid forming β-sheet peptides. In particular, the authors developed small 7-residue de novo peptides, alternating apolar and polar residues (e.g. Ac-Ile-His-Ile-His-Ile-Gln-Ile-$NH_2$, Figure 3A), capable of self-assembling in the presence of Zn(II) ions and forming amyloid-like fibrils.[119,120] The resulting amyloid assemblies acted as effective esterase mimics, catalyzing *p*NPA hydrolysis ($k_{cat} = 0.026 \pm 0.004\ s^{-1}$; $K_m = 0.4 \pm 0.1$ mM; $k_{cat}/K_m = 62 \pm 2\ M^{-1}\ s^{-1}$ for the best candidate, Figure 3B).[120] In addition to homomeric peptide assemblies, heteromeric aggregates were also prepared by mixing different de novo amyloid sequences, for evaluating the effect of specific interactions within the fibrils on their hydrolytic activity.[121] For this purpose, several analogues of a selected heptapeptide were developed, by introducing either positively or negatively charged residues. Interestingly, this study showed that several factors play key roles in affecting the catalytic activity of the de novo amyloid sequences: charge complementarity between the mixed sequences and even small modifications of the peptide structure, such as variation in the side-chain length, may both alter the catalytic performances. To capture and lock such synergistic interactions within de novo amyloid fibrils, the heteromeric constructs were further stabilized by introducing linkers between the β-sheet fragments, leading to self-assembling β-hairpins. Moreover, macrocyclic structures were also developed by placing a linker at each end of the peptide, allowing a precise control of the functional group locations, relative to each other.[122] This strategy was revealed to be effective in promoting

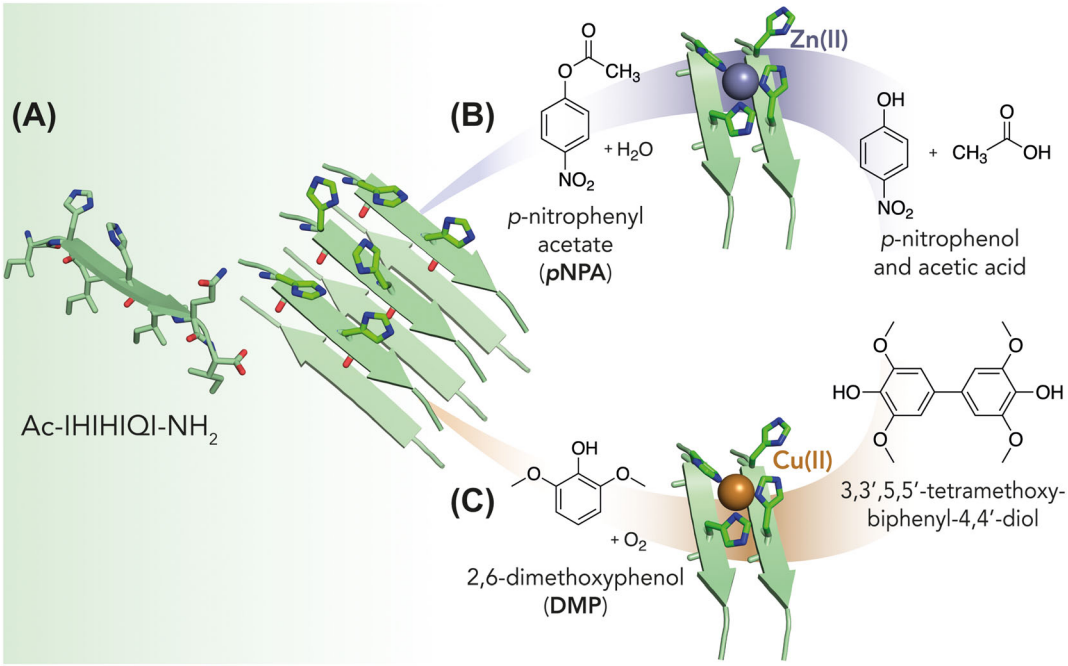


**FIGURE 3** De novo designed catalytic amyloids. A minimal de novo sequence (A) is capable of forming catalytic nanostructures in the presence of metal ions. In particular, when it binds zinc (B), it promotes the hydrolysis of NPA. The same construct, when binding copper (C), catalyzes the oxidation of DMP by activating dioxygen. The model was generated with PyMOL, starting from the ssNMR structure coordinates of the analogue peptide: Ac-Ile-His-Val-His-Leu-Gln-Ile-$NH_2$ (PDB ID: 5UGK).[119]

faster fibril formation, preserving, or enhancing the hydrolytic activity of the individual peptides in the constrained structures.

Korendovich's group expanded the catalytic versatility of this peculiar amyloid-based scaffold beyond hydrolytic activity. Remarkably, a straightforward metal substitution from zinc to copper afforded a catalytic system capable of promoting the oxidation of dimethoxyphenol (DMP) in the presence of dioxygen (Figure 3C).[123] Indeed, mononuclear copper sites are found in enzymes involved in oxygen binding and activation in the frame of numerous biochemical processes.[105,106] Prominent examples of these metalloproteins are Cyt c oxidase (CcO),[124] lytic polysaccharide monooxygenases (LPMO),[125] galactose oxidase,[126] amine oxidase,[127] and the above described CuNiR.[102] While most of these enzymes contain a T2Cu center, CcO, and LPMOs contain more peculiar sites. CcOs contain a unique type of copper center, referred to as $Cu_B$, consisting of a trigonal pyramidal copper site close to a heme center.[124] LPMOs, instead, contain a peculiar structural motif named as "histidine brace", involving the N-terminal amino group and the imidazole $N^{\delta}$ coordination by the N-terminal histidine.[125] Despite their differences, all these enzymes share some distinctive structural features. Copper is usually five-coordinated, with two or three His residues and one or two solvent molecules that are easily displaced for binding dioxygen or hydrogen peroxide. At least one of the coordinating histidines binds copper through its $N^{\varepsilon}$ nitrogen, while all histidines use their $N^{\delta}$ for coordinating copper in electron transfer centers.

In this context, the Chakraborty's group reported the de novo design of a tris-His coordinated artificial Cu peptide (ArCuP), [3SCC-(I9H)$_3$], as a functional model for peroxide activation and its reduction to $H_2O$ ($H_2O_2 + 2e^- + 2H^+ \rightarrow 2H_2O$).[128] Spectroscopic analyses demonstrated that the peptide was capable of binding copper, forming a T2Cu environment. Electrocatalytic experiments led to determining the catalytic parameters ($K_m[H_2O_2] \sim 3$mM and $k_{cat} = 0.72\ s^{-1}$ at pH 7.5), assessing the peroxidase activity of the new ArCuP enzyme. The reactivity of ArCuP was further recently expanded to activate C−H bonds of model organic substrates.[129]

A new and still underexplored area in de novo protein design is represented by the identification of metalloenzymes tailored for hydrogen evolution reactions (HERs). Whereas binuclear binding sites are more prevalent (drawing inspiration from natural [NiFe] or [FeFe] hydrogenases),[130] designs of mononuclear binding sites aimed at this purpose are still uncommon in artificial systems.

Chakraborty and his team have followed this path for constructing artificial hydrogenase (ArH) metalloenzymes, able to catalyze $H_2$ production in environmentally benign conditions. The first studies focused on engineering a tetrahedral $Cys_4$ nickel binding site into a natural copper-binding protein.[131] Recently, the authors described the construction of a de novo designed ArH relying on the self-assembly of two stranded coiled coils (2SCCs) featuring Cys-Xxx-Xxx-Cys motifs on each peptide strand to build the $NiCys_4$ site.[132] The activity toward photocatalytic hydrogen evolution reaction was investigated using a Ru(II) complex as a photosensitizer and ascorbic acid as a sacrificial electron donor. $H_2$ was produced under photocatalytic conditions in a pH-dependent manner. In an effort to enhance the catalytic activity, Chakraborty and co-workers de novo designed a new system, namely 4SCC, having a dual Ni(II)$Cys_4$ site.[133] Even though designed to be a four-stranded coiled coil, 4SCC was mainly present as a trimer in the *apo* form, while in the presence of nickel ion, the equilibrium shifted toward the formation of the dimer and monomer. The

remaining monomer was then trapped by free Ni(II) to give more dimer, until Ni(II) consumption. When tested for hydrogen production, 4SCC resulted in slightly more active than 2SCC; however, the activity was pH dependent as well, and highest at pH 5.5. The different oligomeric states, observed with respect to the design, could be ascribed to disruption of the Van der Waals packing interactions essential for generating precise oligomeric structures, upon introduction of the coordinating residues. Although these models showed modest catalytic activity, they had a significant impact on the de novo design of innovative artificial metalloproteins catalyzing a crucial energy process, such as hydrogen evolution.

Before delving into the principal examples of mononuclear sites active in electron transfer, provided below, it is worth mentioning that designed peptides housing mononuclear iron sites, named UFsc (Uno Ferro single-chain)[134] will be discussed in section 3 of this review, as they are derived from the DF (Due Ferri) artificial diiron proteins.

## 2.2 | Artificial metalloproteins housing mononuclear electron-transfer sites

While successful de novo designs of artificial metalloenzymes incorporating both a structural and a catalytic metal binding site have been spectacularly achieved,[90,96] combining an electron transfer and a catalytic center within the same artificial peptide scaffold remains an unreported challenge. With the goal of replicating such complexity found in nature,[104] we believe that examples of de novo designed artificial mononuclear electron-transfer (ET) proteins deserve mention in this review.

Among ET proteins, several research groups have endeavored to model the coordination site of natural rubredoxins (Rds) within artificial peptide scaffolds. Rds are small (45–60 residues) metalloproteins holding a mononuclear iron site coordinated by four Cys residues (Fe(Cys)$_4$) in a distorted tetrahedral environment.[135] Their structure is characterized by a $C_2$-pseudo-symmetric fold, comprising two conserved Cys-Xxx-Xxx-Cys-Xxx motifs in α-turns.[136] The rigid coordination environment allows the redox cycling of the iron ion, providing stabilization to both Fe(II) and Fe(III) oxidation states.

One of the first examples of de novo designed Rd mimic with redox activity was reported by DeGrado and coworkers. They prepared an artificial rubredoxin, named RM1 (Rubredoxin Mimic 1), a single chain construct, using a dimeric miniRM peptide as a template.[137] They fused the two monomers of miniRM with a highly stable hairpin motif, the tryptophan zipper, and obtained a 40-residue peptide with a different topology from that of the natural protein. Spectroscopic studies demonstrated that RM1 binds transition metal ions in a tetrahedral tetrathiolate coordination geometry, consistent with the design. Remarkably, the iron complex of RM1 was able to perform at least 16 reversible redox cycles under aerobic conditions and was characterized by a midpoint potential of 55 mV, which is at the top edge of the range (−50 mV to 50 mV) reported for bacterial rubredoxins.[135,138]

Despite RM1 behaves as a functional mimic of rubredoxin, its dimensions (40 amino acids) are still close to those of the natural counterpart. With the aim of developing a minimal Rd model, Seneque and coworkers identified an 18-residue fragment capable of reproducing structural and spectroscopic features of the FeCys$_4$ site of *Clostridium pasteurianum* (*Cp*) Rd.[139] The small de novo peptide, named $L_{ZR}$, comprises an 8-residue cyclic structure with a 10-residue linear tail. Both the cyclic and the linear segments contribute to metal binding, each with a Cys-Xxx-Xxx-Cys motif. Notably, the NMR solution structure of Zn(II) $L_{ZR}$ closely matches the crystal structure of Zn-substituted *Cp* Rd. Even more remarkably, the Fe$L_{ZR}$ complex could undergo eight consecutive oxidation–reduction cycles with high yields. This result is particularly significant because it represents the smallest peptide-based rubredoxin model capable of sustaining reversible redox activity. Further, Fe$L_{ZR}$ is characterized by a reduction potential of 144 mV, which surpasses those reported for natural rubredoxins[135,138] and is currently the highest among their designed mimics. This high reduction potential was ascribed to the hydrophilic environment given by polar residues close to the metal site in the $L_{ZR}$ scaffold, which stabilizes the reduced state.

In the same context, focusing on the structural unit of Rubredoxin (Rd) and making use of its intrinsic symmetry, our group developed synthetic rubredoxins models through a miniaturization approach. First, the minimum unit needed to reproduce the Rds metal site was identified by retrostructural analysis.[140] Then, this was used to generate a minimal peptide scaffold, named METP (Miniaturized Electron Transfer Protein; Figure 4). METP is made up of a β-hairpin undecapeptide with two properly spaced Cys residues that self-assembles in the presence of a coordinating metal ion to form a $C_2$ symmetric tetrathiolate binding site. The characterization by several spectroscopic techniques showed that METP avidly binds Co(II), Zn(II), Fe(II), and Fe(III), in the expected 2:1 stoichiometry. The geometry around the metal ion was found to be as designed, resembling the Rd tetrahedral environment. Even though the minimal METP scaffold was a suitable structural model of the natural counterpart, being able to coordinate both Fe(II) and Fe(III) with the expected Rd-like tetrahedral Cys$_4$ geometry, it was unable to perform reversible redox cycles. An autoredox reaction may account for the observed instability of the Fe(III)-tetrathiolate complex, with Fe(III) reduction to Fe(II), and disulfide formation.

With the aim of achieving a redox-active metalloprotein, we have recently focused our design efforts on constructing a more robust, single-chain version of METP, named METPsc1.[141] Starting from the high-potential *Cp Rd* mutant V44A, we engineered METPsc1 in a stepwise design process. First, a 13-residue fragment was extracted from the parent protein, bearing the conserved Cys-Xxx-Xxx-Cys coordinating motif. A $C_2$ symmetry operation was applied to generate a dimeric construct, similar to the METP prototype. Further, a properly designed loop was introduced for linking the N-terminus of the monomeric fragment with the C-terminus of its symmetry-related copy. Finally, a fixed-backbone design was performed to optimize side-chain packing, leading to the 28-residue sequence of METPsc1. The newly designed mini protein was thoroughly characterized in solution, and, notably, the X-ray crystal structure of its zinc complex was in perfect agreement with the designed model. Electrochemical analysis revealed that the FeMETPsc1 showed a reduction potential ($E'^{0} = 121$ mV vs

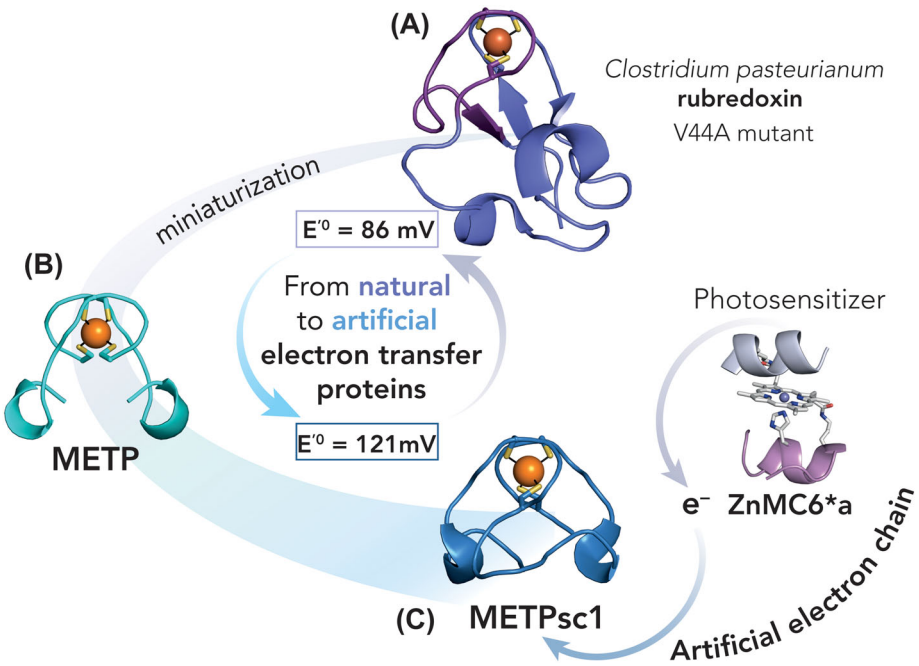


**FIGURE 4** De novo design and miniaturization strategies were used by our group to develop artificial rubredoxin models. Starting from the natural *Clostridium pasteurianum* rubredoxin (A; PDB ID: 1C09), METP[140] was first designed (B) and then a single-chain artificial metalloprotein, METPsc1 (PDB ID: 5SBG),[141] was engineered (C). An artificial electron chain was obtained by coupling METPsc1 to a photosensitizer (ZnMC6*a). Cysteine residues are depicted as sticks and iron ions as orange spheres.

*SHE*), surpassing the classical range for prokaryotic rubredoxins,[138] and closely matching the potential of rubrerythrins.[142] FeMETPsc1 exhibited redox activity for more than 12 consecutive cycles, without any loss in signal upon recycling. Furthermore, the good agreement between the crystal structure and the designed model demonstrated that the designed second-shell interactions were crucial in determining one of the highest potentials amongst the Rd family. This result laid the foundation for the development of a fully synthetic electron transfer chain, from a sacrificial electron donor (TEA) to a sacrificial acceptor ($O_2$), by matching FeMETPsc1 with another synthetic mini enzyme (ZnMC6*a) acting as photosensitizer. Our research opens new perspectives for studying more complex electron transfer chains and may also represent a great opportunity for developing miniaturized proteins for use in optoelectronics and light harvesting. It can provide a starting point for creating multi-component mini-protein devices on a nanoscale level.

Encouraged by these results, in a parallel study, we focused our attention on exploring the ability of the METP scaffold to host different metal binding sites. In this context, we developed a new METP analogue (METP3) by converting the $Cys_4$, rubredoxin-like binding site, into a $Cys_2His_2$ binding site.[143] Few changes in the sequence of METP were needed for preserving the tetrahedral geometry of the metal site upon modification of the first-coordination sphere ligands. METP3 demonstrated the ability to self-assemble into a homodimeric structure in the presence of divalent metal ions (Co(II), Zn(II), and Cd(II)) with the desired tetrahedral geometry. METP3 represents the first example of an artificial metalloprotein housing a mononuclear $Cys_2His_2$ zinc-binding site. It establishes the suitability of the small METP scaffold for accommodating different tetrahedral metal binding sites, regardless of the first coordination sphere ligands.

In an elegant contribution, Pecoraro and coworkers described the design of a new Rd mimic[144] by re-engineering $\alpha_3$DIV.[145] The latter is a construct based on the $\alpha_3$D scaffold and contains three cysteine residues at the C-terminal end. The incorporation of a fourth cysteine residue led to $\alpha_3$DIV-L21C, housing a tetra thiolate metal binding site. Once reconstituted with Fe(II) under anaerobic conditions, $\alpha_3$DIV-L21C displayed the same spectroscopic properties of native rubredoxin, despite utilizing a secondary structure significantly different from the canonical pair of Cys-Xxx-Xxx-Cys motifs found in the α-turn region of the native protein. In a recent paper, the same peptide was successfully reconstituted with molybdenum.[146] The spectroscopic characterization performed on Mo-$\alpha_3$DIV-L21C confirmed the presence of Mo mainly in a Mo(IV) oxidation state. Furthermore, the electrochemical results showed a formal redox potential quite similar to that of Mo-rubredoxin.[147]

Alongside Rds, cupredoxins represent an important class of electron-transfer proteins in Nature. Among them, Blue Copper proteins stand out for their remarkable characteristics, particularly their unconventional coordination geometries. These proteins hold a T1Cu center, in which the Cu(II) ion is situated within a trigonal plane defined by two His residues and one Cys ligand ($His_2Cys$), accompanied by one or two weakly interacting axial ligands, resulting in either a trigonal pyramidal or trigonal bipyramidal geometry.[148] In an effort to replicate this binding environment, Tanaka and coworkers, de novo designed a four-stranded coiled coil scaffold capable of coordinating Cu(II) in a trigonal geometry, dictated by a $His_2Cys$ binding site, as in natural cupredoxins.[149] The blue copper site was designed within the hydrophobic core of the protein to prevent water coordination to the copper ion. This would have a dual effect: (i) it would stabilize a T1 Cu site with respect to a T2 Cu site; (ii) it would disfavor the Cu(II) oxidation state, thus avoiding disulfide bond formation upon Cu(II) reduction to Cu(I). The resulting model, named AM2C (Figure 5A), was capable of binding copper, and cycling between Cu(I) and Cu(II) oxidation states. The observed redox potential ($E_{1/2}$)

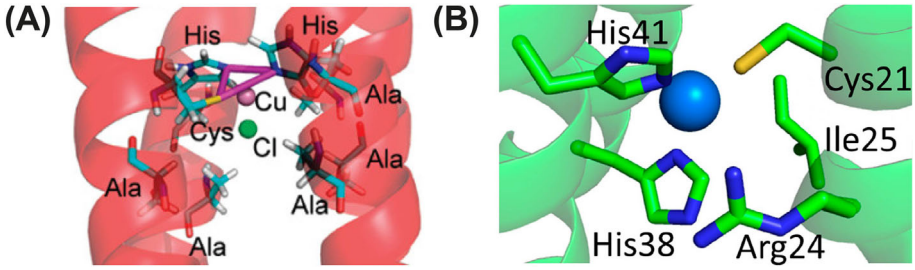


**FIGURE 5** Structure of T1 Cu sites in de novo designed blue copper proteins. (A) AM2C model, adapted with permission from reference.[149] *Copyright: © 2010, American Chemical Society.* (B) GR$\alpha_3$DChC5 model, adapted from reference.[150] *Copyright: © 2020, American Chemical Society.*

was 328 mV vs NHE, close to that of natural Azurin (305 mV vs NHE).[151] While this similarity supported the classification of AM2C as a new Type 1 Blue Copper artificial protein, the observed $K_d$ value for AM2C (2.1 μM) was significantly higher if compared to that of the Azurin-Cu(II) complex (25 fM).[152] Further investigations, involving amino acid mutations may be necessary to address this difference. When AM2C was designed, only the trigonal plane formed by the two histidines and the cysteine in the cavity of the scaffold was considered; hence, the space for an exogenous ligand was still available. In a subsequent paper, the same group exploited this vacancy to force the trigonal planar geometry toward a tetrahedral-like one, by using different ligands (chloride, phosphate, sulfate, acetate, azide, and imidazole).[153] The study of the spectroscopic features of the new metalloenzyme was performed, leading to a new example of Green Copper artificial protein,[154] named AM2CE1, having an unusual tetrahedral-like geometry, and bearing an imidazole as the axial ligand.

Blue Copper proteins have also been a source of inspiration for the de novo design studies of Pecoraro and his research team. The anti-antiparallel three-helix bundle scaffold $\alpha_3$D, was engineered to house an electron transfer site, resulting in three constructs: $\alpha_3$D-CR, $\alpha_3$D-CH, $\alpha_3$D-ChC (CR = core; CH = chelate; ChC = chelate core).[155] $\alpha_3$DIV,[156] already able to bind heavy metals, was used as a scaffold, and the symmetric $Cys_3$ site was mutated in a transition metal $His_2$-CysMet binding site (as found in plastocyanin and rusticyanin).[105] Among all CR and CH constructs,[155] which mostly produced T2Cu sites as highlighted by spectroscopic properties, the electron transfer activity of Cu$\alpha_3$D–CH3 was studied using five different photosensitizers.[157] A 400 nm absorption band in the transient UV–vis spectra of Cu$\alpha_3$D–CH3 indicated the formation of a Cu(II) species, as desired, and the complete depletion of the photo-oxidant, suggesting the involvement of the copper center in an electron transfer reaction. If AM2C (Blue Copper protein) was converted in AM2CE1 (Green Copper protein) exploiting ligands exchange, Pecoraro and his team successfully achieved the task of traversing the red-green-blue color spectrum within the same rationally designed cupredoxin model, GR$\alpha_3$DChC (where $\alpha_3$D is further stabilized with an additional heptad).[150] GR$\alpha_3$DChC2 was found to be a red copper-like protein with a $His_2$CysGlu copper binding site, due to an unexpected interaction of copper ion with a surface $Glu^{41}$.[158] Mutation studies of GR$\alpha_3$DChC2 resulted in a green copper protein (GR$\alpha_3$DChC4) and a blue copper one (GR$\alpha_3$DChC5, Figure 5B). Remarkably, this was the first instance where binding site tuning of cupredoxins models was achieved without the use of exogenous ligands.

## 3 | PEPTIDE SCAFFOLDS HOUSING MULTINUCLEAR BINDING SITES

A wide number of metalloenzymes contain multinuclear metal clusters to accomplish catalytic functions or serve as electron- or proton-delivery systems.[104,159] Multinuclear sites have been engineered into peptide-based models in order to elucidate the main features controlling the activity of natural metal clusters and, ultimately, to construct synthetic enzymes with tailored properties.[28,65] Substantial part of these enzymes contain dinuclear metal cofactors, which in turn could be either homonuclear or heteronuclear. In this section, we will describe prominent examples of artificial metalloproteins hosting dinuclear and multinuclear metal sites, designed by drawing inspiration from natural systems.

### 3.1 | Dinuclear binding sites

Diiron centers are the most abundant dinuclear metal sites and are found in a class of metalloproteins referred to as bacterial multicomponent monooxygenases (BMMs).[160,161] Among them, the most studied are methane monooxygenases (MMOs), which activate molecular oxygen to catalyze the insertion of an oxygen atom into the exceptionally stable C-H bond of methane.[162–165] The hydroxylase component holds the dinuclear iron site, where oxygen activation and substrate oxygenation take place. The first coordination sphere of the diiron site is composed of two histidines and four glutamates, two of which are bridging the two metal ions. The diiron site coordination and geometry, as well as the nature and relative orientations of surrounding residues, are highly maintained within the BMMs family. They are also similar to those found in other carboxylate-bridged diiron enzymes, including functionally divergent proteins, such as ferritins[166] and ribonucleotide reductases.[167] Further, the diiron site is housed within a conserved four-helical coiled coil or four-helix bundle.[168,169]

A prominent example of de novo designed metalloproteins containing a diiron metal binding site within a four-helix bundle is the "Due Ferri" (two-irons; DF) family, jointly developed by the DeGrado's and our group. DF design was aimed at reproducing the structural and functional properties of diiron oxidases and oxygenases in a small and compact peptide scaffold.[170] The first model, named DF1 (Figure 6A), is a homodimer consisting of two 48-residue helix–loop–helix ($\alpha_2$) peptide chains, self-assembling into an

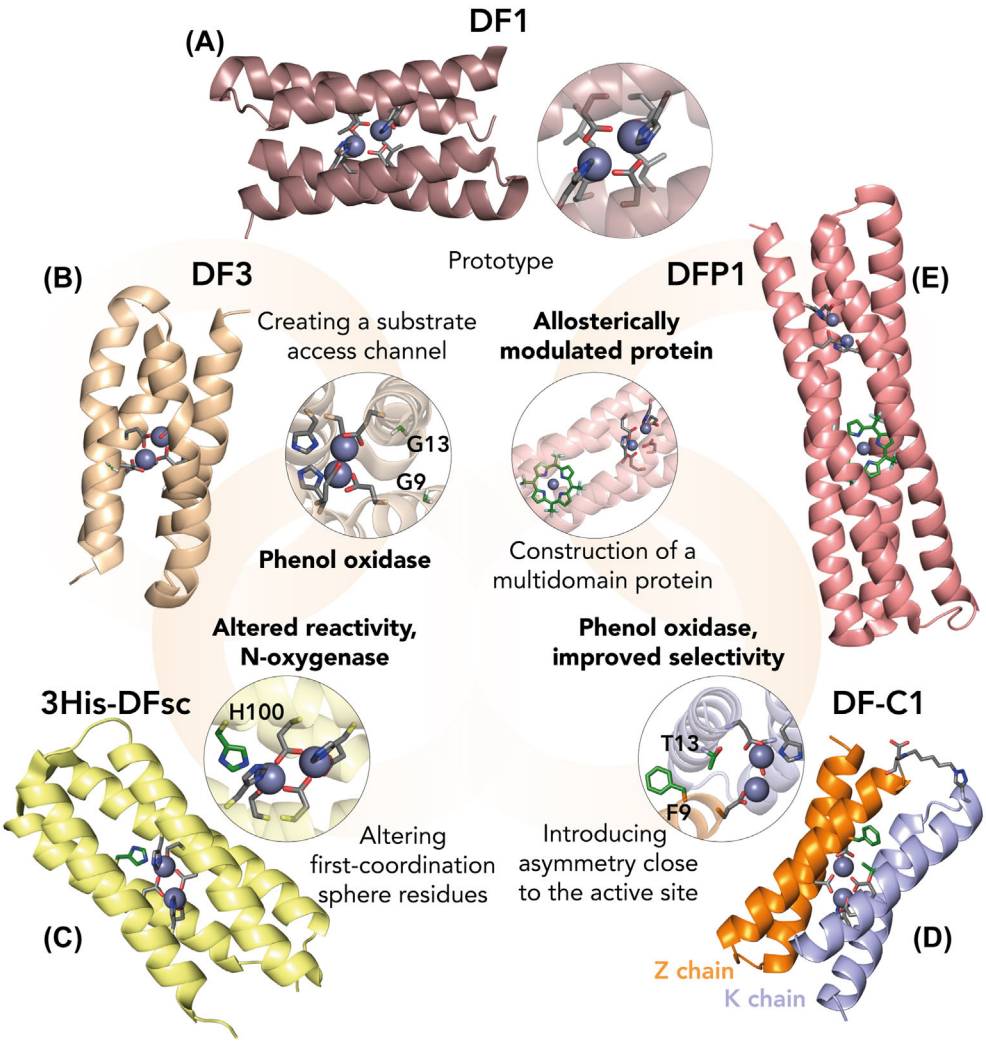


**FIGURE 6** Structures of DF proteins with details of the metal-binding sites. In the insets, the most significant mutations introduced in DF analogues are labeled and depicted as green sticks. (A) X-ray crystal structure of the prototype model, DF1 (PDB ID: 1EC5).[171] (B) NMR structure of DF3 (PDB ID: 2KIK).[172] (C) NMR structure of the 3His-G2DFsc variant (PDB ID: 2LFD).[173] (D) Designed model of the hetero-dimeric DF-C1.[174] (E) X-ray crystal structure of the multidomain protein DFP1 (PDB ID: 7JH6).[175]

antiparallel four-helix bundle.[171] In each $\alpha_2$ subunit, one helix bears a Glu-Xxx-Xxx-His motif as found in natural proteins, where a bridging Glu residue is in the *a* position and a terminal His is in *d* position of the coiled coil. An additional Glu residue is placed in the other helix of each $\alpha_2$, providing the fourth ligand to each metal ion. DF1 was highly stable, well-folded, and able to bind divalent metal ions in the intended metal:protein ratio. Further, DF1 is the first protein, entirely designed from scratch, for which both crystallographic and NMR structures were obtained.[171,176] Although DF1 behaved as a native-like protein, as it was designed to maximize the bundle stability, its tightly packed peptide scaffold did not allow access for substrates, preventing any kind of functionality. Therefore, the four Leu residues close to the metal site were mutated to either Ala or Gly, to open a channel for binding of small substrates in the DF1 mutants.[177,178] However, these mutations decreased the buried surface area of the helical bundle, thus decreasing the overall stability of the protein. These findings highlight that destabilizing effects are necessary to achieve functionality, both in designed as well as in native metalloproteins.[176] In order to optimize the scaffold for catalytic activity, a combinatorial approach was adopted, in which the effects of systematic mutations on metal binding, substrate binding, and catalytic properties were evaluated. The $O_2$-dependent oxidation of 4-aminophenol (4-AP) to 4-benzoquinone monoimine (4-BQM) was selected as a test reaction to investigate the ability of the artificial proteins to activate dioxygen while cycling between the diferrous and the diferric state. For this screening, a series of asymmetric hetero tetrameric four-helix bundles ($DF_{tet}$) were generated by self-assembly of disconnected helices. The 24-residue helices of DF1 were elongated to 33 residues, offering an extended hydrophobic interface driving the folding of the coiled coil.[179] Further, an automated algorithm was developed to identify the interactions stabilizing the desired topology and those destabilizing other possible topologies, using an approach termed as negative design.[180] The construct containing four glycine residues in the proximity of the metal site (G4-$DF_{tet}$) displayed the highest affinity toward the phenol substrate and exhibited the most rapid initial rate of 4-AP oxidation to 4-BQM, achieving a ≈ 1,000-fold enhancement compared to the background reaction. The diferric complex of G4-$DF_{tet}$ oxidized 4-AP with a saturation kinetics as natural enzymes, thus allowing for the determination of the catalytic parameters through Michaelis–Menten analysis ($k_{cat} = 1.3 \pm 0.1$ $min^{-1}$; $K_m = 0.83 \pm 0.06$ mM; $k_{cat}/K_m = 1.5$ $mM^{-1}$ $min^{-1}$).[180]

Studies on the $DF_{tet}$ subset clearly provided precious insights into the active site requirements for function. However, the tetrameric assemblies were not amenable to structural characterization. As four glycines were revealed to be crucial for substrate accessibility, these mutations were introduced in the homodimeric assembly. In this case, a redesign of the $\alpha_2$ loop of DF1 was necessary to balance the destabilization induced by the introduction of the helix-breaking glycine residues. The resulting protein, named DF3 (Figure 6B), behaved as an efficient phenol oxidase and is the first de novo designed catalytic metalloprotein to be structurally characterized by NMR.[172,181] Particularly, DF3 displayed a 2-fold increased $k_{cat}$ (2.7 ± 0.2 $min^{-1}$), despite 2.5-fold increased $K_m$ (2.0 ± 0.3 mM) with respect to G4-$DF_{tet}$, yielding a nearly unchanged catalytic efficiency ($k_{cat}/K_m = 1.4$ $mM^{-1}$ $min^{-1}$). The expanded active site of DF3 was able to host even a larger substrate, and to catalyze the oxidation of 3,5-di-tert-butyl-cathecol (DTBC) to the corresponding quinone (DTBQ), with saturation kinetics, similar to alternative oxidase and plastid terminal oxidase[182] ($k_{cat} = 13.2 \pm 1.2$ $min^{-1}$; $K_m = 2.1 \pm 0.3$ mM; $k_{cat}/K_m = 6.3$ $mM^{-1}$ $min^{-1}$, ambient $O_2$).[172]

A step further in the design process consisted in the modulation of the second sphere and long-range interactions, with the aim of inducing and controlling reaction selectivity. Natural enzymes exert this kind of fine control by means of an asymmetric protein environment surrounding the active site. One approach to the design of less symmetric proteins involved the construction of a monomeric single-chain version of DF proteins (DFsc). DFsc was designed as a 114-residue protein consisting of four helices and three interconnecting loops.[183] Accurate design of the loop sequences was essential to provide the protein with a robust scaffold, able to tolerate multiple mutations. Several variants of the DFsc protein were developed, first aimed at optimizing the substrate access channel for 4-AP oxidation,[184] and then to completely alter the $O_2$-dependent reactivity.[173,185,186] Particularly, redesign of the first coordination sphere was directed to mimic the active site of *p*-aminobenzoate N-oxygenase (AurF), which is the only structurally characterized diiron protein displaying this kind of reactivity. Accordingly, a third His was included as a ligand to the diiron center, as found in AurF, and a series of additional mutations in the second and third coordination spheres were introduced to create a hydrogen bond network stabilizing the buried polar residue in the hydrophobic core.[173] Notably, the resulting proteins, named 3His-G4DFsc and 3His-G2DFsc (Figure 6C) selectively catalyzed the N-oxygenation of arylamines, similarly to AurF. Furthermore, the dizinc complex of 3His-G2DFsc was able to bind and stabilize the semiquinone radical ($SQ^{\cdot-}$) formed from an equimolar mixture of DTBC and DTBQ.[187] Stabilization of reactive species in the protein interior is a mechanism generally adopted by metalloenzymes to fully control their reactivity avoiding side reactions, thus represents a benchmark in de novo protein design.

The prominent role of the peptide scaffold in determining this remarkable property was further established by altering the metal binding site of DFsc from a binuclear to a mononuclear iron center through the substitution of one bridging glutamate with a histidine. The mononuclear metal-binding analog, namely UFsc (Uno Ferro single-chain), was still able to stabilize the $SQ^{\cdot-}$ radical upon binding of a single equivalent of Zn(II) with a comparable yield to di-Zn(II)-3His-G2DFsc.[134] In a further study, UFsc was used to generate a library of analogues for screening the effect of punctual mutations on the affinity toward several divalent cations.[188] This study provides a full description of how the metal binding selectivity of a peptide scaffold can be finely tuned by rationally designed mutations. Indeed, altering the nature and the size of ligands in the first and second coordination spheres results in improved selectivity toward a specific divalent cation.

Recently, the promiscuity of DF proteins toward binding of different metal ions was expanded beyond divalent cations, and the dititanium(IV) complex of DFsc was reported.[189] Notably, DFsc scaffold effectively modulates the reactivity of Ti(IV) ions, promoting hydrolytic cleavage of DNA over uncontrolled hydrolysis.

The construction of asymmetric DF proteins was also achieved through an alternative strategy involving covalent ligation of two $\alpha_2$ subunits. Starting from the observation of natural toluene monooxygenase (TOMO),[190] asymmetry was implemented by introducing specific mutations in the scaffold of DF3. In particular, two of the four glycines were mutated to Thr and Phe in the inner and outer regions of the substrate access channel, respectively, to favor specific recognition of phenolic substrates. The resulting $\alpha_2$ peptide chains were then modified to introduce clickable functionalities. The use of azide- and alkyne-modified amino acids enabled the incorporation of functional groups during the solid phase synthesis of peptides, avoiding any subsequent functionalization.[191] This method yielded the first heterodimeric DF protein, named DF-C1 (DF-Click1, Figure 6D).[174] DF-C1 not only was able to catalyze 4-AP oxidation to 4-BQM but also stabilized this reactive product in the protein interior, promoting its oxidative dimerization. The lack of hydrogen peroxide detection upon 4-AP oxidation further indicated that DF-C1 promoted the net four-electron reduction of dioxygen to water, preventing the release of reactive intermediates in solution. These results represent an important step forward in the design of de novo proteins capable of promoting complex transformations in a selective and controlled manner, closely resembling natural metalloenzymes. Altogether, studies on DF proteins demonstrate the power of the de novo design approach in developing functional enzymes. Lowering the complexity found in natural systems allows for better control of the factors directing metal cofactor reactivity, highlighting how simple mutations in the active site can completely repurpose metalloprotein function and dictate reaction selectivity.

Laying on these solid foundations, De Grado and our groups have recently constructed an allosterically regulated metalloprotein by fusing together two de novo designed protein domains.[175] One of them is based on DF1, while the other domain consists of PS1 (porphyrin-binding sequence), a four-helix bundle protein capable of binding an artificial Zn-porphyrin cofactor (ZnP).[192] Since DF1 and PS1 possess different bundle architectures, a computational method was developed to find the most designable helical connections suitable for bridging the two topologies. The resultant protein, named DFP1 (Figure 6E), was a single-chain four-helix bundle retaining the cofactor

binding properties of the separate domains, as confirmed by its crystal structure, in perfect agreement with the design. Allosteric modulation was expected to operate across the multidomain protein, as the binding of ZnP causes structural and dynamic changes in PS1, which should impact the catalytic activity of the fused DF domain. As DFP1 was designed for the highest thermodynamic stability, some mutations in its tightly packed core were introduced to achieve functionality. In particular, in DFP2 four glycines replaced leucines and alanines at the positions lining the substrate access cavity to the active site, as in DF3. Both DFP1 and DFP2 existed in a monomer-dimer equilibrium, possibly due to the formation of an elongated domain-swapped dimer.[193] Redesign of the interhelical loop with a helix-breaking sequence led to DFP3, which was mostly monomeric also in the absence of cofactors. DFP3 behaved as an allosterically modulated phenol oxidase. Indeed, the diiron form of DFP3 performed 4-AP oxidation with saturation kinetics in the absence of ZnP, exhibiting a slightly increased $K_m$ (2.9 ± 0.3 mM) and decreased $k_{cat}$ (0.70 ± 0.04 $min^{-1}$) and catalytic efficiency ($k_{cat}/K_m = 0.24$ $mM^{-1}{\cdot}min^{-1}$) compared to DF3.[172] The corresponding ZnP-bound diiron DFP3 protein also showed Michaelis–Menten oxidation kinetics, but the catalytic parameters were significantly influenced by the binding of the allosteric modulator ZnP, resulting in a 4-fold higher $K_m$ (0.68 ± 0.15 mM) and a 7-fold decreased $k_{cat}$ (0.11 ± 0.01 $min^{-1}$), corresponding to an overall lowered catalytic efficiency ($k_{cat}/K_m$ of 0.16 $mM^{-1}{\cdot}min^{-1}$).[175] The design strategy adopted for the construction of DFP-fused proteins not only proved successful in preserving the structural and functional properties of the original proteins but also in enabling allosteric communication between the domains. This study represents a milestone in protein design, offering a general approach for the assembly of complex molecular machineries and allosterically regulated multi-domain proteins.

A rather peculiar diiron site is found in [FeFe]-hydrogenases, which catalyze reversible proton reduction to form hydrogen ($H_2$).[194,195] The diiron site is part of a remarkably complex metal cofactor known as the H-cluster, which is formed by two redox-coupled iron sites. One is an iron–sulfur cubane cluster, named [4Fe4S]H, similar to those found in some ferredoxins and other electron transfer proteins, while the other is named [2Fe]H, and it is where hydrogen formation or splitting takes place. The coordination sphere composition of the [2Fe]H cluster is uncommon among metalloproteins. It consists of two iron ions connected by a 2-aza-propane-(1,3)-dithiolate (ADT) and a CO molecule as bridging ligands. In addition, each iron ion is coordinated by another CO molecule and a $CN^-$ anion. One of the two irons (called proximal iron $Fe_p$) is also bound to a thiolate from a cysteine sidechain, which is shared with the [4Fe4S]H cofactor, making it six-coordinated, while the other iron ion (distal iron or $Fe_d$), contains one vacancy to coordinate hydrogen.[196] Despite the inner complexity of their metal cofactor, [FeFe]-hydrogenases have been privileged targets for bioinorganic chemists, aiming at reproducing their unique structural and catalytic properties into peptide-based architectures. Countless synthetic mimics of the hydrogenase diiron site have been reported, mostly in the form of small molecule complex.[197,198]

Early work in this field was focused on anchoring synthetic dithiolate bridged diiron hexacarbonyl complexes to peptide scaffolds. The first peptide-based structural model of [FeFe]-hydrogenases was reported by Dutton and coworkers, which consisted of a de novo helical peptide able to bind the diiron cluster through cysteine residues.[199] The peptide-metal complex displayed spectroscopic features matching those of the natural metalloproteins, but no redox activity was reported. Subsequently, other research groups have constructed [FeFe]-hydrogenase mimics employing either synthetic or natural peptides containing dithiols to bind the diiron core. Weigand and coworkers inserted diiron hexacarbonyl complex into the disulfide bond of the cyclic peptide drug Sandostatin®, and studied the structural and redox properties of the complex. Although the peptide-diiron complex was not stable in aqueous solution, it was able to perform electrochemical proton reduction in DMF.[200] Jones and coworkers adopted a different approach to connect a diiron core to a peptide scaffold without using thiolates as anchoring sites. They added to the peptide sequence, an artificial phosphine amino acid to replace a terminal CO molecule of the metal cluster.[201] Since alkyl phosphines have a larger electron-donating capacity than CO, they act as better mimics of $CN^-$ found in hydrogenases. As a result, the phosphine-bound dithiolate bridged diiron pentacarbonyl complex showed improved electrocatalytic properties compared to previously reported synthetic analogues. Furthermore, Hayashi and coworkers developed a photocatalytic peptide-based system for hydrogen production based on a peptide fragment derived from cytochrome $c_{556}$.[202] In this study, the 18-residue peptide served as a scaffold to covalently bind both the diiron carbonyl core and a photoactive ruthenium complex through the Cys-Xxx-Xxx-Cys-His heme-binding motif. In particular, the native heme coordinating histidine was chosen as the anchoring site for the ruthenium photosensitizer, and the two cysteines acted as ligands for the diiron hexacarbonyl complex. Notably, the intramolecular system promoted light-driven hydrogen evolution from water, although displaying a limited turnover number.

A hetero binuclear metal cofactor is found in [NiFe]-hydrogenases, which represent the most common type of hydrogenases.[203,204] These enzymes hold a biologically unusual metal binding site in which a nickel ion is tetracoordinated by four cysteine thiolates, two of them bridging with a Fe $(CO)(CN)_2$ moiety. While several mimics of the [FeFe]-hydrogenases diiron cluster have been reported, catalytic models of [NiFe]-hydrogenases are rare and consist of small molecule synthetic complexes.[205] Structural mimics of [NiFe]-hydrogenases exhibit negligible activity, highlighting the essential role that the protein environment plays in defining the metal cofactor properties. The first peptide-based model of [NiFe]-hydrogenases was reported by Dutta and coworkers, adopting a minimalist approach. In this work, the N-terminal nickel-binding 7-residue fragment derived from the enzyme nickel superoxide dismutase (NiSOD) was chosen as a template for building heteronuclear metal complexes.[206] As in the parent enzyme, nickel is coordinated by the N-terminal amine, an amide nitrogen from the peptide backbone, and two cysteine thiolates which represent bridges to the additional metal site. The exchange of labile ligands from various metal complexes with the peptide-derived

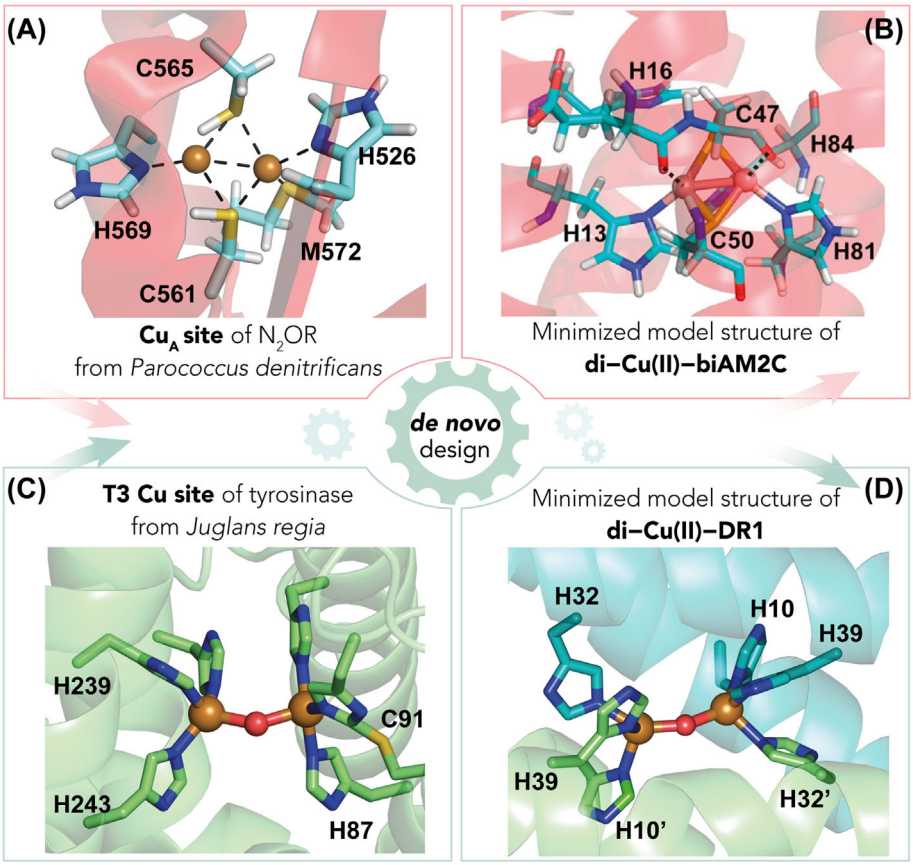


**FIGURE 7** Structure of dinuclear copper sites in natural and de novo designed metalloproteins. (A) $Cu_A$ site of nitrous oxide reductase from *Parococcus denitrificans* (PDB ID: 1FWX) compared to (B) di-Cu(II)-biAM2C model. Adapted with permission from reference.[210] *Copyright: © 2012 American Chemical Society*. (C) Type 3 copper site of tyrosinase from *Juglans regia* (PDB ID: 5CE9) compared to (D) di-Cu(II)-DR1 model.[211]

thiolates provided an efficient general method for the synthesis of heteronuclear complexes with different nature and nuclearity, opening the gate to the construction of elaborated metal cofactors into minimal peptide scaffolds.

Very recently, Falkoski, Nanda, and coworkers developed a minimalist di-nickel binding peptide as a functional hydrogenase model.[207] In this study, a homo dinuclear metal site was engineered by taking inspiration from the nickel site of [NiFe]-hydrogenases. Since in the latter proteins, the nickel coordinating cysteines are far in the sequence, the authors surveyed the PDB to find a short, continuous, metal-binding motif able to accommodate nickel in its preferred coordination geometries. A 12-residue fragment (Cys-Xxx-Cys-Gly-Cys-Xxx-Xxx-Xxx-Xxx-Xxx-Cys-Gly) was identified and then the variable positions were defined through structure-guided design. The resulting nickelback (NB) model was able to bind nickel in a 2:1 metal-to-peptide ratio, featuring a coordination geometry similar to that found in [NiFe]-hydrogenases and closely resembling the di-nickel cluster of acetyl-CoA (coenzymeA) synthase. The di-Ni-NB complex was able to promote photocatalytic hydrogen production from water upon matching with Eosin Y as photosensitizer and triethanolamine (TEOA) as a sacrificial electron donor. Remarkably, this mini-enzyme performed 500 turnovers, surpassing previously reported nickel-containing artificial hydrogenases.[208,209]

In addition to diiron sites, dicopper sites are also diffused among natural metalloproteins. For example, dinuclear copper clusters are found in purple $Cu_A$ cupredoxins (Figure 7A), which include cytochrome c oxidase (CcO) and nitrous oxide reductase ($N_2OR$).[212] These are electron transfer proteins involved in essential processes such as aerobic and anaerobic respiration.[213] Cupredoxins have been compelling targets for bioinorganic chemists, aiming at replicating the coordination geometries found in their metal sites, which are not preferred by copper in any oxidation state. They are usually classified based on their deep colors, resulting from charge-transfer bands.[148] The mononuclear T1 site of Blue Copper proteins has been discussed in section 2.2. The dinuclear copper cluster of purple cupredoxins is bridged by two cysteine thiolates from a conserved Cys-Xxx-Xxx-Xxx-Cys sequence, forming a $Cu_2S_2$ diamond structure. Each copper ion is additionally coordinated by a histidine and a weakly coordinating endogenous or exogenous ligand. Copper ions are constrained in a fixed coordination geometry by a rigid protein environment, which typically consists of a Greek key arrangement of β-sheets.[214] Following their previous studies on mononuclear cupredoxin models[149,153] (see section 2.2), Tanaka and coworkers succeeded in implanting a $Cu_A$ purple site into a de novo designed four-helix bundle.[210] The single-chain metalloprotein AM2C[153] served as a template, in which two cysteines and two histidines essential for $Cu_A$ coordination were introduced. The resulting construct, named di-Cu(II)-biAM2C (Figure 7B) displayed typical absorption and EPR features of purple cupredoxins, which decayed with a half-life of 2.4 h due to cysteine oxidation. These results indicate that a binuclear copper site could be engineered in a completely different folding compared to that found in the natural protein. Further, it is worth to note that no significant

steric constraints were necessary to reproduce the rigid coordination environment of cupredoxins in the α-helical scaffold.

Dinuclear copper centers, referred as type 3 copper sites (T3Cu), are found in several proteins committed to $O_2$ transport, as hemocyanin, or its activation for catalyzing oxidative transformations.[215] The latter enzymes are usually defined as polyphenol oxidases (PPOs) and include both monophenolase and diphenolase enzymes. Monophenolase activity is typical of tyrosinases, which possess the unique ability to perform hydroxylation of monophenolic substrates. Conversely, diphenolase activity consists of the oxidation of a catechol substrate. The active site of T3Cu proteins consists of two copper ions, each coordinated by three histidine residues (Figure 7C). Each histidine triad derives from an antiparallel α-helical pair, enclosing the metal site in a four-helix bundle. The coordination and geometry of the active site are highly conserved among T3Cu proteins, and the structural basis for either mono or diphenolase activity is still under debate.[216,217] The absence of protein-derived bridging ligands provides an additional level of complexity to the reconstruction of T3Cu centers into artificial peptide scaffolds. Recently, our group has faced this challenge and developed the first T3 copper containing de novo protein, named DR1 (Due Rame: two copper, Figure 7D).[211] Starting from the crystal structure of DF1, the first coordination sphere was remodeled to convert the $Glu_4His_2$ diiron binding site into a $His_6$ dicopper binding site. As described for the design of 3His-DFsc, additional mutations were introduced to optimize second-shell interactions and create a hydrogen bond network spanning from the binding site through the helical bundle. Spectroscopic and catalytic analysis showed that DR1 properly hosts a T3Cu site into the designed helical bundle and behaves as a functional diphenolase enzyme. Remarkably, the modeled interactions within the protein active site enable to discriminate among different catechol derivatives, endowing DR1 with substrate selectivity proper of native enzymes.[211]

## 3.2 | Multinuclear metal sites

All the examples reported in the previous section emphasize the significant progress achieved in the design of peptide-based scaffolds binding dinuclear metal cofactors. Multinuclear clusters represent attractive candidates for researchers since they are employed by natural enzymes to promote some of the most difficult chemical transformations relevant for life. Among them, multicopper oxidases (MCOs) perform the oxidation of several substrates coupled to the four-electron reduction of dioxygen to water.[218,219] In doing this, a mononuclear T1Cu center serves as an electron acceptor from the substrate, then transfers the reducing equivalents far apart to a trinuclear copper cluster, where dioxygen reduction occurs. Multicopper clusters are found also in metallothioneins,[220] a family of cysteine-rich metalloproteins involved in copper homeostasis and protection against toxic elements, given their high affinity toward $d^{10}$ metal ions.

The design of multicopper sites was described by Ogawa and coworkers, who reported the Cu(I) binding properties of a designed four-helix bundle with spectroscopic properties resembling those of natural metallothioneins.[221,222] Further, the same group reported the design of a three-helix bundle binding a tetra-Cd(II) cluster arranged in a tetrahedral adamantane-like geometry coordinated by a Cys-Xxx-Xxx-Cys-Glu motif.[223]

Iron-sulfur (FeS) clusters are among the most widespread electron transfer centers within biological systems.[224] This prevalence stems from the incorporation of abundant reserves of iron and sulfur atoms into early proteins during the anaerobic conditions of Earth's first billion years.[225] These metal cofactors are indeed involved in a broad range of life processes, acting as redox mediators in metabolic, mitochondrial respiratory, and photosynthetic pathways.[226–228] The simplest kind of iron-sulfur cluster is the mononuclear $FeCys_4$ metal center of rubredoxins, which has been described in section 2.2, dedicated to mononuclear binding sites. Among multinuclear sites, the [4Fe-4S] is the most ubiquitous form.[229] These cofactors are commonly found in purely electron transfer proteins, named ferredoxins, but are also integrated as electron delivery modules in complex enzymes, such as hydrogenases[230,231] and photosystem I (PSI).[232] This motif is characterized by four iron ions and four sulfide anions placed at the vertices of a cubane-type cluster. The Fe centers are typically further coordinated by cysteinyl thiolate ligands.

The assembly of artificial electron transport chains for their potential application in energy-related catalysis has stimulated great interest in the design of peptide scaffolds hosting [4Fe-4S] clusters. As mentioned for cupredoxins and rubredoxins, major challenges have to be faced in designing [4Fe-4S] proteins. Indeed, metal binding sites of iron-sulfur proteins commonly contain loops and β-sheet structures,[224] while α-helical scaffolds have been generally preferred in designed metalloproteins because of their high designability and tolerance to multiple mutations. Early studies were directed at identifying the essential requirements that enable the incorporation of the [4Fe-4S] cofactor in natural ferredoxins. These proteins are characterized by a common α/β fold, which binds the cubane cluster through four cysteines in a conserved sequence (Cys-Xxx-Xxx-Cys-Xxx-Xxx-Cys-$[Xxx]_n$-Cys). Following this minimalist approach, Dutton and coworkers developed the first prototype of ferredoxin maquette (FdM), consisting of a 16-aminoacid sequence derived from *Peptococcus aerogenes* ferredoxin I.[233,234] Later, several FdM mutants were developed, serving as convenient models for screening the effect of mutations on cluster formation and its redox activity.[235,236] These studies provided valuable insights into ferredoxin chemistry, elucidating that the exact cysteine spacing in the consensus cluster-forming sequence is an essential requisite for cluster formation while highlighting the role of non-binding amino acids in cofactor redox modulation.[235,236] Later, Mitchell and coworkers revisited FdMs and explored their integration in a semi-synthetic electron transfer process.[237] Starting from a poly-glycine sequence bearing appropriately spaced Cys residues, tuning of the cluster reduction potential was pursued by switching a thiolate ligand of one cysteine with the selenolate of a selenocysteine (Sec), but little changes were observed among the screened sequences. Notably, the synthetic [4Fe-4S] maquettes were coupled to [FeFe]-hydrogenase CaHydA from

*Clostridium acetobutylicum*, effectively replacing its natural ferredoxin partner in $H_2$-oxidation.

Noy and coworkers were the first to transplant the [4Fe-4S] into a fully α-helical de novo scaffold, using a strategy termed as "metal first approach".[238] First, they identified a minimal helical fragment from the protein *Thermatoga maritima* tryptophanyl-tRNA synthase, which contains the [4Fe-4S] center within three helical elements.[239] One of the helices containing a Cys-Xxx-Xxx-Cys motif was chosen as the starting point for the design of the four-helix bundle. Then, by extending the cluster symmetry to the entire protein scaffold, a coiled coil iron-sulfur protein was designed (named CCIS1), containing two of these motifs at an appropriate distance to bind the [4Fe-4S] cluster. Though the protein was able to properly host the metal cofactor, it was unable to perform reversible redox cycles, possibly because of sulfur hydrolysis upon reduction of the cluster. Several variants of the CCIS scaffold were also reported, displaying improved cofactor binding, and achieving a single oligomeric state.[240]

While previously mentioned examples describe isolated iron-sulfur clusters, Ghirlanda, and coworkers were the first to incorporate multiple [4Fe-4S] cofactors within de novo helical bundles.[241] In doing this, they exploited the formation of domain-swapped dimers (DSD). In DSD, two identical peptides form helical hairpins, each consisting of one helix that is double the length of the other.[193] The hairpins dimerize in an antiparallel orientation, where the short helices link each other end-to-end and pair with the long helices forming a three-helix bundle. This arrangement resembles that found in two-cluster ferredoxins, which are characterized by two-fold internal symmetry. Mirroring the active site of these proteins, three of the four coordinating cysteines were provided by one monomer, while the fourth came from the other monomer. Despite the large dimensions of the clusters, CD analysis of the apo (DSD-4Cys) and holo dimer (DSD-bis[4Fe-4S]) revealed that the secondary structure was not significantly altered upon cofactor incorporation, indicating preorganized metal binding sites.[241] DSD-bis[4Fe-4S] displayed two clusters at the predicted distance of ~30 Å, as confirmed by spectroscopic studies. Since this distance is too far for studying efficient electron transfer, the authors developed a second generation of DSD bearing two clusters within a biologically relevant distance for effective electron transfer processes.[242] Starting from the DSD-4Cys model, the metal binding sites were moved by one heptad toward the center along the bundle's longitudinal axis. The resulting model, named DSD-Fdm (Figure 8A) was able to host two clusters with a 12 Å separation and represents the first de novo [4Fe-4S] protein able to perform reversible redox cycles, with a reduction potential ($E'^0 = -479$ mV vs *SHE*) in the range of natural low-potential ferredoxins.[244] Further, the authors probed the ability of DSD-Fdm to effectively transfer electrons to a natural redox protein, promoting the reduction of oxidized cytochrome *c*. These findings show that coupling these two

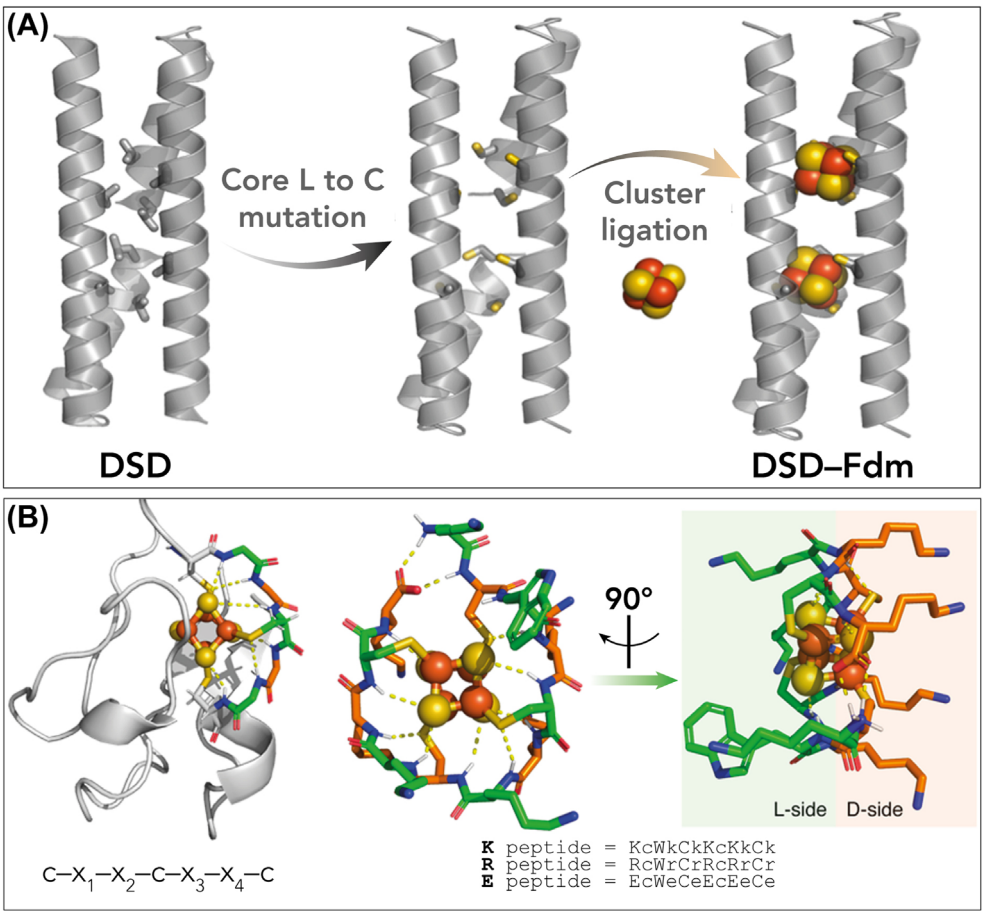


**FIGURE 8** Examples of de novo designed [4Fe-4S]-binding proteins. (A) Stepwise design of DSD-Fdm. Adapted with permission from reference.[242] *Copyright: © 2014, American Chemical Society*. (B) Structure-based design of ambidoxins, starting from the identification of the minimal cluster-binding sequence in natural ferredoxins, and then its reconstruction in a de novo sequence consisting of alternating L (uppercase) and D (lowercase) amino acids. Adapted with permission from reference.[243] *Copyright: © 2018, American Chemical Society*.

[4Fe-4S] clusters within a de novo peptide scaffold resulted in the formation of a redox-active electron transfer center, which could potentially be used as part of an artificial system for catalysis or synthetic biology applications. FdMs and [4Fe-4S]-binding helical coiled coils all share the use of a fragment sequence found in natural proteins as the basis for their design.

Falkowski, Nanda, and coworkers approached the challenge with a different strategy, aiming to replicate the structural features rather than cluster-forming sequences of natural ferredoxins (Figure 8B).[243] Their design started with a conformational analysis of the iron-sulfur binding heptapeptide sequence (Cys-Xxx-Xxx-Cys-Xxx-Xxx-Cys) in the structures present in the PDB, which showed a common pattern alternating alpha-left ($\alpha_L$) and alpha-right ($\alpha_R$) backbone conformations. Based on this observation, this structural motif was extended to a 12-residue peptide sequence, resulting in a peculiar, curved backbone wrapping around the [4Fe-4S]-cluster. This unusual fold was achieved using alternating L and D amino acids, which stabilize the $\alpha_R$ and $\alpha_L$ backbone conformation, respectively, and was further stabilized by hydrogen bonds between backbone amides and cysteine thiolates or sulfides from the cluster. For this reason, this minimal ferredoxin mimic was termed as "ambidoxin". Three ambidoxin variants were produced, containing either basic (lysine in the K peptide, arginine in the R peptide) or acidic (glutamic acid in the E peptide) amino acids in all the positions not occupied by cysteines. Iron–sulfur cluster assembly was observed only with the positively charged peptides, named K and R, whereas it was not observed for the negatively charged E peptide. In this last case, electrostatic destabilization of the 4Fe−4S−4(Cys) complex, bearing a − 2 or −3 charge depending on the oxidation state, would presumably hamper cluster assembly. Importantly, the K and R ambidoxins not only displayed spectroscopic and redox properties ($E'^{0} = -450$ mV vs *SHE*) closely matching those of bacterial ferredoxins[244] but were able to perform over 1,000 reversible redox cycles, exhibiting superior robustness compared to any artificial ferredoxin model.[243]

One of the ultimate goals of metalloprotein design is the integration of artificial enzymes in biological systems. To this end, cofactor reconstitution *in vivo* is essential and still remains a crucial task. Only a few examples of in vivo metalloprotein assembly have been reported, and involved a covalent binding with the cofactor, such as with heme *c*.[245]

Nanda and coworkers have tackled this challenge in a recent work, by attempting reconstitution of CCIS protein in *E. coli*.[246] Previous studies on this scaffold highlighted that the oligomerization state of CCIS was variable and strongly dependent on the conditions of the in vitro reconstitution protocol.[240] Surprisingly, in vivo reconstitution of CCIS led to a single oligomeric state corresponding to a trimer instead of the expected monomer. This trimeric CCIS was still incorporating a single [4Fe-4S]-cluster, but its chemical properties were significantly altered compared to those of the in vitro assembled protein. In particular, the cluster exhibited slightly improved oxygen tolerance and a higher resistance to reduction by dithionite, indicating a more negative reduction potential compared to ferredoxins.[246] Mutagenesis studies provided useful insights into the reconstitution mechanism, but there is still limited mechanistic understanding of how cluster assembly occurs. This study represents a starting point for in vivo biogenesis of artificial metalloproteins and their integration into living cells.

Whereas a number of models have been obtained using cysteines or inorganic sulfur as bridging ligands, the design of multinuclear centers with oxygen-rich ligands has been much less diffused, despite their significance to enzymes involved in essential biological processes. Indeed, one of the most prominent examples of multinuclear metal sites found in living systems is the $Mn_4Ca$ cluster of photosystem II (PSII), promoting the four-electron oxidation of two water molecules to form dioxygen.[247] The $Mn_4Ca$ cluster is arranged in a distorted cuboidal geometry, bridged by five oxygen atoms, and bound to the protein by seven amino acid residues (Figure 9A). Due to its unique properties, it has been the subject of extensive spectroscopic and structural characterization,[249–252] inspiring the design of artificial catalysts for water oxidation.[253]

De Grado and our groups have tackled the challenge of assembling for the first time a fully carboxylate-bridged tetranuclear metal cluster into a de novo designed peptide scaffold[248,254] (Figure 9B). Starting from a symmetric antiparallel four-helix bundle, the tetranuclear cluster was engineered by introducing specific mutations with respect to the active site of DF proteins. In the newly designed proteins, named 4DH1 and 4DH2, the glutamate residues of DF were replaced with the shorter aspartates to widen the metal binding site, enabling the accommodation of a tetranuclear cluster. Moreover, two additional histidines were introduced as metal ligands. Strong hydrophobic packing interactions were modeled at both ends of the helical bundle to stabilize the global structure, allowing the insertion of the metal cluster in the protein core.[248] Notably, the stabilization of hydrophilic metal binding residues in the protein interior was achieved through the construction of an extended hydrogen bond network, including second- and third-shell H-bonds. This study represents a crucial step forward in the development of synthetic analogues of the oxygen-evolving complex and other elaborated multinuclear metal clusters.

Structural and functional similarities observed between the $Mn_4Ca$ cluster of PSII and the $Mn_2$ cluster of manganese catalase stimulated the researchers to develop artificial proteins holding a dinuclear manganese binding site, as a basis for understanding the complex chemistry performed by the $Mn_4Ca$ center in PSII. Although they cannot replicate the four oxidation steps, dinuclear Mn complexes exhibit some features of the $Mn_4Ca$ cluster, including the ability to perform catalytic oxygen formation. Along these lines, the Allen group developed a series of dimanganese-binding artificial proteins and tested their reactivity in one of the key steps of photosynthesis.[255] Due to the complex nature of PSII, they selected the bacterial reaction center from *Rhodobacter sphaeroides* as the target and investigated the ability of their de novo proteins to bind and reduce the oxidized bacteriochlorophyll dimer ($P_{865}^{+}$), which is the primary electron donor in photosynthetic bacteria. For these studies, Allen and coworkers used the structure of the homodimeric four-helix bundle DF2t as a template.[256] The first protein (P0) shared the same

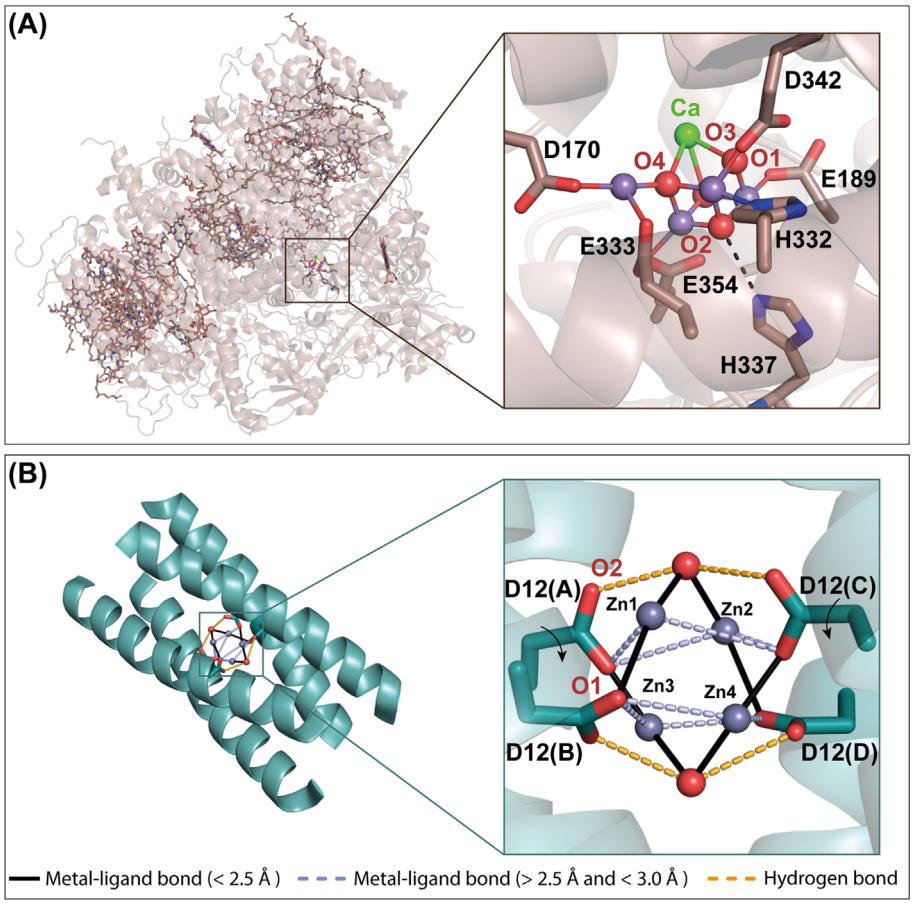


**FIGURE 9** (A) X-ray crystal structure of photosystem II from *Thermosynechococcus elongatus* (PDB ID: 1SL5) with a detail on the oxygen-evolving $Mn_4Ca$ cluster. (B) X-ray crystal structure of the de novo designed 4DH1 model (PDB ID: 5WLL), with a detail of the $Zn_4$ cluster.[248]

sequence of DF2t, housing a dinuclear manganese center in the middle of the helical bundle.[255] Further design was devoted to engineering additional $Mn_2$ binding sites in the outer regions, close to the connecting loops. Due to the symmetry of the P0 protein dimer, introducing Mn-binding ligands far from the center results in two dinuclear sites with identical sets of ligands that are symmetrically located at equal distances from the center. Accordingly, the analog named P1 was characterized by three $Mn_2$ binding sites. Conversely, the central metal site was replaced with hydrophobic residues in P2, thus retaining only the two outer binding sites of P1. Spectroscopic studies evidenced that all the de novo proteins promoted electron transfer to $P_{865}^+$, with P1 displaying the highest efficiency.[257] The relative effectiveness of the three proteins correlates with the number of $Mn_2$ centers since a higher number of metal sites increases the possibility of electron transfer. However, it could be due to other parameters, such as different reduction potentials between the central and outer metal sites, or the distance between the Mn cofactor and $P_{865}^+$ when the protein is bound to the reaction center. This study represents an example in which de novo metalloproteins have been integrated into biological machinery, highlighting the ability of artificial proteins to replace natural components in complex enzymatic systems. Furthermore, Allen and coworkers expanded the array of $Mn_2$-binding metalloproteins, shifting the position of the outer metal binding site still further from the center of the bundle. Due to their close similarity with the Mn catalase metal site, all these proteins were tested for their ability to promote hydrogen peroxide disproportionation to $O_2$ and $H_2O$.[257] A detailed kinetic analysis showed that the catalytic efficiency depended on the number of dimanganese sites but not on their position. Interestingly, P1 protein displayed a $K_m$ for $H_2O_2$ similar to that of native Mn catalase, but significantly lower $k_{cat}$ value, prompting future design toward engineering of second-shell interaction favoring substrate activation.

## 4 | CONCLUSIONS

In this review, we have illustrated the impressive progress made over the last 20 years in designing peptide-based artificial metalloproteins. By collecting significant examples of peptide scaffolds housing mononuclear and multinuclear metal sites, we have highlighted the great potential of de novo design and miniaturization approaches in reproducing the structural features of natural metalloproteins and in providing them with electron transfer or catalytic activity.

Despite the huge amount of literature concerning the design of heme protein mimics,[258–260] we have decided to focus on the engineering of metal sites, characterized by an increased level of complexity compared to heme centers. Indeed, in the design of non-heme centers, the coordination requirements of the metal site must be fully satisfied by the protein ligand, seeking the balance between thermodynamic stability and flexibility, essential for functionality.

Although mononuclear metal sites may appear simple, there is considerable complexity lying outside of the first coordination sphere, which has not been yet thoroughly explored or understood.

In this context, an inestimable contribution has been given by Pecoraro and coworkers, who were the first to recreate the $ZnHis_3$ site of carbonic anhydrase within α-helical peptide structures.[90] Their pioneering work has inspired several other research groups, who have implanted the CA site within different de novo scaffolds, affording artificial hydrolases. Remarkably, the TRI-based CA mimic displays only 500-fold lower $CO_2$ hydration activity compared to the fastest CA isoform, which is still unparalleled among artificial metalloenzymes. The same scaffold was shown to effectively host a redox-active copper center, producing an efficient CuNiR mimic, without the need for modulation of secondary sphere interactions.[91] Controlling interactions beyond the first coordination sphere has been achieved in CA models by stammer insertion,[110] and then by directed evolution. In this respect, Hilvert and coworkers have recently demonstrated the power of this technique for the optimization of a de novo designed metalloprotein (MID1sc),[113] succeeding not only in enhancing its hydrolytic activity but also in introducing enantioselectivity and expanding its reactivity toward abiotic transformations.[114] Conversely, modeling secondary interactions has been widely pursued in artificial rubredoxin models. Lessons learned from the extensive mutagenesis studies on natural rubredoxins have been transplanted and upgraded in their peptide-based mimics, achieving the modulation of reduction potential beyond the limits observed for natural counterparts.[139,141]

Moving from single to multiple metal sites, the equilibrium between stability and flexibility in the host peptide scaffold becomes even more delicate and challenging to achieve. The DF family of four-helix-bundle metalloproteins, developed by DeGrado and our groups, represents a paradigm of the most widely adopted approach for the construction of functional multinuclear metalloproteins. This strategy starts with the construction of a prototype model, endowed with the highest stability and carefully reproducing the active site structure of the parent protein. Such a model was then subjected to an iterative re-design process, in which some mutations were introduced to achieve functionality, and others were needed to balance the consequent destabilization. The initial design was facilitated by the nearly symmetric nature of the inspiring metal cluster found in natural diiron-containing metalloproteins. Indeed, once identified the peptide sequence for binding one of the two iron ions, a symmetry-related copy could be easily generated, yielding a homodimeric structure housing the diiron site. Similar considerations can be extended to more complex metal centers, such as [4Fe-4S] clusters, which have been engineered into highly symmetric peptide scaffolds, as domain-swapped dimers[242] and coiled coils.[238] However, different from iron-sulfur clusters, which are purely electron-transfer centers, the protein matrix in diiron enzymes has the power to dictate substrate specificity and product selectivity. These properties, typical of native enzymes, have been introduced in the DF scaffold by breaking the symmetry while moving further from the active site. This extraordinary level of control has been achieved by generating hetero-tetrameric ($DF_{tet}$),[179] single-chain (DFsc),[183] and heterodimeric (DF-C1) proteins,[174] in which secondary interactions, including hydrogen bond networks and steric bulk modulation, have been successfully designed. Finally, the DF scaffold has also served as a template for shaping different functionalities, by altering the nature of the metal ions and/or changing the ligands in the primary coordination sphere.[173,189,211,255]

In summary, all the examples reported in this review unequivocally illustrate that peptide-based scaffolds are excellent candidates for "getting married" with metal ions and constructing an "inclusive family" of artificial, functional metalloproteins.

Looking at the future, we believe that combining rational design and directed evolution approaches will be effective for developing robust artificial metalloenzymes tailored for any desired activity. We are also confident that the current computational tools will be powered by machine-learning-based methods, improving the speed and accuracy of model prediction. Even though it is not easy to foresee in which direction this research field will move, we expect that the following pathways will be explored. One route involves the design of stable, robust, and easily tailorable peptide-based nanomaterials. This actually represents a rapidly growing research trend, which aims at merging the advantages of both enzymatic and heterogeneous catalysts.[261,262] Compared to inorganic nanomaterials, peptide-based nanostructures are inherently biodegradable and can function in biocompatible conditions. Prominent examples reported in this review have demonstrated the great potential of amyloid fibrils, which can be designed to bind multiple metal sites, promoting tandem catalysis.[80,120,123] Another pathway involves in vivo production of artificial metalloproteins capable of functioning in whole cells. Indeed, aside from a few exceptional cases reported so far,[246] some breakthroughs would be required to reach this goal, as whole-cell transformations represent future methods for the synthesis of high-added value compounds. With these challenges and opportunities in mind, we envision that precise and accurate metalloprotein design will enable us to obtain customized biocatalysts for satisfying a wide range of social needs.

## ACKNOWLEDGEMENTS

The authors wish to thank all coworkers for their contributions to the results described in this review. M.D.F and A.E. thank the Italian Ministry of University and Research (MUR) for being awarded a research associate (PONR&I 2014-2020, CUP: E65F21003010003) and a Ph. D. (PONR&I 2014-2020, CUP: E65F21003750003) position, respectively. L.L. is grateful to the European Research Council (ERC) for being granted a research associate position in the frame of the "BioDisOrder" project (UGOV 000005_HORIZON2020_ERC_2018_BioDisOrder). Part of the authors' work described in this review was supported by Italian MUR, PRIN 2020, Project SEA-WAVE 2020BKK3W9, [CUP E69J22001140005]. The authors finally acknowledge the Italian MUR program "Dipartimenti di Eccellenza 2023-2027" for the projects arCHIMede [CUP E63C22003710006]. Open Access funding was provided by the University of Naples Federico II, within the CRUI-CARE WILEY Agreement.

## ORCID

*Linda Leone* https://orcid.org/0000-0001-7293-1814
*Maria De Fenza* https://orcid.org/0000-0002-2856-5615
*Alessandra Esposito* https://orcid.org/0009-0007-7099-6359
*Ornella Maglio* https://orcid.org/0000-0002-7829-1907
*Flavia Nastri* https://orcid.org/0000-0002-3390-9822
*Angela Lombardi* https://orcid.org/0000-0002-2013-3009


## REFERENCES


1. Huang P-S, Boyken SE, Baker D. The coming of age of de novo protein design. *Nature*. 2016;537(7620):320-327. doi:10.1038/nature19946
2. Korendovych IV, DeGrado WF. De novo protein design, a retrospective. *Q Rev Biophys*. 2020;53:e3. doi:10.1017/S0033583519000131
3. Chalkley MJ, Mann SI, DeGrado WF. De Novo metalloprotein design. *Nat Rev Chem*. 2022;6(1):31-50. doi:10.1038/s41570-021-00339-5
4. Khakzad H, Igashov I, Schneuing A, Goverde C, Bronstein M, Correia B. A new age in protein design empowered by deep learning. *Cell Syst*. 2023;14(11):925-939. doi:10.1016/j.cels.2023.10.006
5. Ferruz N, Heinzinger M, Akdel M, Goncearenco A, Naef L, Dallago C. From sequence to function through structure: deep learning for protein design. *Comput Struct Biotechnol J*. 2023;21:238-250. doi:10.1016/j.csbj.2022.11.014
6. Behrendt R, White P, Offer J. Advances in Fmoc solid-phase peptide synthesis. *J Pept Sci*. 2016;22(1):4-27. doi:10.1002/psc.2836
7. Jad YE, Kumar A, El-Faham A, De La Torre BG, Albericio F. Green transformation of solid-phase peptide synthesis. *ACS Sustain Chem Eng*. 2019;7(4):3671-3683. doi:10.1021/acssuschemeng.8b06520
8. Jaradat DMM, Musaimi OA, Albericio F. Advances in solid-phase peptide synthesis in aqueous media (ASPPS). *Green Chem*. 2022;24(17):6360-6372. doi:10.1039/D2GC02319A
9. Sinha NJ, Kloxin CJ, Saven JG, Jensen GV, Kelman Z, Pochan DJ. Recombinant expression of computationally designed peptide-bundlemers in Escherichia Coli. *J Biotechnol*. 2021;330:57-60. doi:10.1016/j.jbiotec.2021.03.004
10. Gaglione R, Pane K, Dell'Olmo E, et al. Cost-effective production of recombinant peptides in Escherichia Coli. *New Biotechnol*. 2019;51:39-48. doi:10.1016/j.nbt.2019.02.004
11. Yang J, Anishchenko I, Park H, Peng Z, Ovchinnikov S, Baker D. Improved protein structure prediction using predicted Interresidue orientations. *Proc Natl Acad Sci USA*. 2020;117(3):1496-1503. doi:10.1073/pnas.1914677117
12. Jumper J, Evans R, Pritzel A, et al. Highly accurate protein structure prediction with AlphaFold. *Nature*. 2021;596(7873):583-589. doi:10.1038/s41586-021-03819-2
13. Chowdhury R, Bouatta N, Biswas S, et al. Single-sequence protein structure prediction using a language model and deep learning. *Nat Biotechnol*. 2022;40(11):1617-1623. doi:10.1038/s41587-022-01432-w
14. He S, Bauman D, Davis JS, et al. Facile synthesis of site-specifically acetylated and methylated histone proteins: reagents for evaluation of the histone code hypothesis. *Proc Natl Acad Sci USA*. 2003;100(21):12033-12038. doi:10.1073/pnas.2035256100
15. Manohar M, Mooney AM, North JA, et al. Acetylation of histone H3 at the nucleosome dyad alters DNA-histone binding. *J Biol Chem*. 2009;284(35):23312-23321. doi:10.1074/jbc.M109.003202
16. Unverzagt C, Kajihara Y. Chemical assembly of N-glycoproteins: a refined toolbox to address a ubiquitous posttranslational modification. *Chem Soc Rev*. 2013;42(10):4408-4420. doi:10.1039/c3cs35485g
17. Piontek C, Ring P, Harjes O, et al. Semisynthesis of a homogeneous glycoprotein enzyme: ribonuclease C: part 1. *Angew Chem Int Ed*. 2009;48(11):1936-1940. doi:10.1002/anie.200804734
18. Hejjaoui M, Butterfield S, Fauvet B, et al. Elucidating the role of C-terminal post-translational modifications using protein Semisynthesis strategies: α-Synuclein phosphorylation at tyrosine 125. *J Am Chem Soc*. 2012;134(11):5196-5210. doi:10.1021/ja210866j
19. Agyei D, Tan K-X, Pan S, Udenigwe CC, Danquah MK. 9 - Peptides for Biopharmaceutical Applications. In: Koutsopoulos S, ed. *Peptide applications in biomedicine, biotechnology and bioengineering*. Woodhead Publishing; 2018:231-251. doi:10.1016/B978-0-08-100736-5.00009-0
20. Jimmidi R. Synthesis and applications of peptides and peptidomimetics in drug discovery. *Eur J Org Chem*. 2023;26(18):e202300028. doi:10.1002/ejoc.202300028
21. Zhang P, Cui Y, Anderson CF, et al. Peptide-based nanoprobes for molecular imaging and disease diagnostics. *Chem Soc Rev*. 2018;47(10):3490-3529. doi:10.1039/C7CS00793K
22. Li T, Lu X-M, Zhang M-R, Hu K, Li Z. Peptide-based nanomaterials: self-assembly, properties and applications. *Bioact Mater*. 2022;11:268-282. doi:10.1016/j.bioactmat.2021.09.029
23. Snoj J, Lapenta F, Jerala R. Preorganized cyclic modules facilitate the self-assembly of protein nanostructures. *Chem Sci*. 2024;15(10):3673-3686. doi:10.1039/D3SC06658D
24. Sheehan F, Sementa D, Jain A, et al. Peptide-based supramolecular systems chemistry. *Chem Rev*. 2021;121(22):13869-13914. doi:10.1021/acs.chemrev.1c00089
25. Zozulia O, Dolan MA, Korendovych IV. Catalytic peptide assemblies. *Chem Soc Rev*. 2018;47(10):3621-3639. doi:10.1039/C8CS00080H
26. Koebke KJ, Pinter TBJ, Pitts WC, Pecoraro VL. Catalysis and electron transfer in de novo designed metalloproteins. *Chem Rev*. 2022;122(14):12046-12109. doi:10.1021/acs.chemrev.1c01025
27. Liu Q, Kuzuya A, Wang Z-G. Supramolecular enzyme-mimicking catalysts self-assembled from peptides. *iScience*. 2023;26(1):105831. doi:10.1016/j.isci.2022.105831
28. Nastri F, D'Alonzo D, Leone L, et al. Engineering metalloprotein functions in designed and native scaffolds. *Trends Biochem Sci*. 2019;44(12):1022-1040. doi:10.1016/j.tibs.2019.06.006
29. Klein AS, Zeymer C. Design and engineering of artificial metalloproteins: from de novo metal coordination to catalysis. *Protein Eng Des Sel*. 2021;34:gzab003. doi:10.1093/protein/gzab003
30. Kerns SA, Biswas A, Minnetian NM, Borovik AS. Artificial metalloproteins: at the Interface between biology and chemistry. *JACS Au*. 2022;2(6):1252-1265. doi:10.1021/jacsau.2c00102
31. Crichton R (Ed). *Biological inorganic chemistry: a new introduction to molecular structure and function*. Third Academic Press; 2019. doi:10.1016/B978-0-12-811741-5.00025-4
32. Maglio O, Nastri F, Lombardi A. Structural and functional aspects of metal binding sites in natural and designed metalloproteins. In: *Ionic interactions in natural and synthetic macromolecules*. John Wiley & Sons, Ltd; 2012:361-450. doi:10.1002/9781118165850.ch11
33. Dudev T, Lim C. Competition among metal ions for protein binding sites: determinants of metal ion selectivity in proteins. *Chem Rev*. 2014;114(1):538-556. doi:10.1021/cr4004665
34. Costas M, Mehn MP, Jensen MP, Que L. Dioxygen activation at mononuclear nonheme iron active sites: enzymes, models, and intermediates. *Chem Rev*. 2004;104(2):939-986. doi:10.1021/cr020628n
35. Serrano-Plana J, Garcia-Bosch I, Company A, Costas M. Structural and reactivity models for copper oxygenases: cooperative effects and novel reactivities. *Acc Chem Res*. 2015;48(8):2397-2406. doi:10.1021/acs.accounts.5b00187
36. Friedle S, Reisner E, Lippard SJ. Current challenges of modeling diiron enzyme active sites for dioxygen activation by biomimetic synthetic complexes. *Chem Soc Rev*. 2010;39(8):2768-2779. doi:10.1039/c003079c
37. Gamba I, Codolà Z, Lloret-Fillol J, Costas M. Making and breaking of the O-O bond at iron complexes. *Coord Chem Rev*. 2017;334:2-24. doi:10.1016/j.ccr.2016.11.007

38. Kal S, Xu S, Que L Jr. Bio-inspired nonheme iron oxidation catalysis: involvement of oxoiron(V) oxidants in cleaving strong C–H bonds. *Angew Chem Int Ed*. 2020;59(19):7332-7349. doi:10.1002/anie.201906551
39. Amanullah S, Saha P, Dey A. Recent developments in the synthesis of bio-inspired iron porphyrins for small molecule activation. *Chem Commun*. 2022;58(39):5808-5828. doi:10.1039/D2CC00430E
40. Maglio O, Chino M, D'Alonzo D, et al. Peptide-based artificial metalloenzymes by design. In: *Peptide and protein engineering for biotechnological and therapeutic applications*. World Scientific; 2022:371-420. doi:10.1142/9789811261664_0010
41. Chen K, Arnold FH. Engineering new catalytic activities in enzymes. *Nat Catal*. 2020;3(3):203-213. doi:10.1038/s41929-019-0385-5
42. Jeschek M, Panke S, Ward TR. Artificial metalloenzymes on the verge of new-to-nature metabolism. *Trends Biotechnol*. 2018;36(1):60-72. doi:10.1016/j.tibtech.2017.10.003
43. Vornholt T, Christoffel F, Pellizzoni MM, Panke S, Ward TR, Jeschek M. Systematic engineering of artificial metalloenzymes for new-to-nature reactions. *Sci Adv*. 2021;7(4):eabe4208. doi:10.1126/sciadv.abe4208
44. Hammer SC, Knight AM, Arnold FH. Design and evolution of enzymes for non-natural chemistry. *Curr Opin Green Sustain Chem*. 2017;7:23-30. doi:10.1016/j.cogsc.2017.06.002
45. Fujieda N, Tonomura A, Mochizuki T, Itoh S. Asymmetric Michael addition catalysed by copper–amyloid complexes. *RSC Adv*. 2024;14(1):206-210. doi:10.1039/D3RA07900G
46. Moser CC, Sheehan MM, Ennist NM, et al. Chapter Sixteen - De novo construction of redox active proteins. In: Pecoraro VL, ed. *Methods in enzymology*. Vol.580, Peptide, Protein and Enzyme Design. Academiv Press; 2016:365-388. doi:10.1016/bs.mie.2016.05.048
47. Jeong WJ, Lee J, Eom H, Song WJ. A specific guide for metalloenzyme designers: introduction and evolution of metal-coordination spheres embedded in protein environments. *Acc Chem Res*. 2023;56(18):2416-2425. doi:10.1021/acs.accounts.3c00336
48. Hoffnagle AM, Tezcan FA. Atomically accurate design of metalloproteins with predefined coordination geometries. *J Am Chem Soc*. 2023;145(26):14208-14214. doi:10.1021/jacs.3c04047
49. Lin Y-W. Rational design of metalloenzymes: from single to multiple active sites. *Coord Chem Rev*. 2017;336:1-27. doi:10.1016/j.ccr.2017.01.001
50. Zhu J, Avakyan N, Kakkis A, et al. Protein assembly by design. *Chem Rev*. 2021;121(22):13701-13796. doi:10.1021/acs.chemrev.1c00308
51. Davis HJ, Ward TR. Artificial metalloenzymes: challenges and opportunities. *ACS Cent Sci*. 2019;5(7):1120-1136. doi:10.1021/acscentsci.9b00397
52. Bloomer BJ, Clark DS, Hartwig JF. Progress, challenges, and opportunities with artificial metalloenzymes in biosynthesis. *Biochemistry*. 2023;62(2):221-228. doi:10.1021/acs.biochem.1c00829
53. Lemon CM, Marletta MA. Designer heme proteins: achieving novel function with abiological heme analogues. *Acc Chem Res*. 2021;54(24):4565-4575. doi:10.1021/acs.accounts.1c00588
54. Oohora K, Onoda A, Hayashi T. Hemoproteins reconstituted with artificial metal complexes as biohybrid catalysts. *Acc Chem Res*. 2019;52(4):945-954. doi:10.1021/acs.accounts.8b00676
55. Lewis JC. Beyond the second coordination sphere: engineering dirhodium artificial metalloenzymes to enable protein control of transition metal catalysis. *Acc Chem Res*. 2019;52(3):576-584. doi:10.1021/acs.accounts.8b00625
56. Van Stappen C, Deng Y, Liu Y, et al. Designing artificial metalloenzymes by tuning of the environment beyond the primary coordination sphere. *Chem Rev*. 2022;122(14):11974-12045. doi:10.1021/acs.chemrev.2c00106
57. Mirts EN, Bhagi-Damodaran A, Lu Y. Understanding and modulating metalloenzymes with unnatural amino acids, non-native metal ions, and non-native metallocofactors. *Acc Chem Res*. 2019;52(4):935-944. doi:10.1021/acs.accounts.9b00011
58. Nguyen TK, Ueno T. Engineering of protein assemblies within cells. *Curr Opin Struct Biol*. 2018;51:1-8. doi:10.1016/j.sbi.2017.12.005
59. Marshall LR, Zozulia O, Lengyel-Zhand Z, Korendovych IV. Minimalist de novo design of protein catalysts. *ACS Catal*. 2019;9(10):9265-9275. doi:10.1021/acscatal.9b02509
60. Baker EG, Bartlett GJ, Porter Goff KL, Woolfson DN. Miniprotein design: past, present, and prospects. *Acc Chem Res*. 2017;50(9):2085-2092. doi:10.1021/acs.accounts.7b00186
61. Dawson WM, Rhys GG, Woolfson DN. Towards functional *de novo* designed proteins. *Curr Opin Chem Biol*. 2019;52:102-111. doi:10.1016/j.cbpa.2019.06.011
62. Pan X, Thompson MC, Zhang Y, et al. Expanding the space of protein geometries by computational design of de novo fold families. *Science*. 2020;369(6507):1132-1136. doi:10.1126/science.abc0881
63. Sakuma K, Kobayashi N, Sugiki T, et al. Design of complicated all-α protein structures. *Nat Struct Mol Biol*. 2024;31(2):1-8. doi:10.1038/s41594-023-01147-9
64. Rai J. Mini heme-proteins: designability of structure and diversity of functions. *Curr Protein Pept Sci*. 18(11):1132-1140.
65. Lin Y-W. Rational design of artificial metalloproteins and metalloenzymes with metal clusters. *Molecules*. 2019;24(15):2743. doi:10.3390/molecules24152743
66. Leone L, D'Alonzo D, Maglio O, et al. Highly selective indole oxidation catalyzed by a Mn-containing artificial mini-enzyme. *ACS Catal*. 2021;11(15):9407-9417. doi:10.1021/acscatal.1c01985
67. Leone L, Muñoz-García AB, D'Alonzo D, Pavone V, Nastri F, Lombardi A. Peptide-based metalloporphyrin catalysts: unveiling the role of the metal ion in indole oxidation. *J Inorg Biochem*. 2023;246:112298. doi:10.1016/j.jinorgbio.2023.112298
68. Zambrano G, Sekretareva A, D'Alonzo D, et al. Oxidative dehalogenation of trichlorophenol catalyzed by a promiscuous artificial heme-enzyme. *RSC Adv*. 2022;12(21):12947-12956. doi:10.1039/D2RA00811D
69. D'Alonzo D, De Fenza M, Pavone V, Lombardi A, Nastri F. Selective oxidation of halophenols catalyzed by an artificial miniaturized peroxidase. *Int J Mol Sci*. 2023;24(9):8058. doi:10.3390/ijms24098058
70. Chino M, La Gatta S, Leone L, et al. Dye decolorization by a miniaturized peroxidase Fe-MimochromeVI*a. *Int J Mol Sci*. 2023;24(13):11070. doi:10.3390/ijms241311070
71. Edwards EH, Le JM, Salamatian AA, et al. A cobalt mimochrome for photochemical hydrogen evolution from neutral water. *J Inorg Biochem*. 2022;230:111753. doi:10.1016/j.jinorgbio.2022.111753
72. D'Souza A, Wu X, Yeow EKL, Bhattacharjya S. Designed heme-cage β-sheet miniproteins. *Angew Chem Int Ed*. 2017;56(21):5904-5908. doi:10.1002/anie.201702472
73. D'Souza A, Bhattacharjya S. De novo-designed β-sheet heme proteins. *Biochemistry*. 2021;60(6):431-439. doi:10.1021/acs.biochem.0c00662
74. Nagarajan D, Sukumaran S, Deka G, Krishnamurthy K, Atreya HS, Chandra N. Design of a heme-binding peptide motif adopting a β-hairpin conformation. *J Biol Chem*. 2018;293(24):9412-9422. doi:10.1074/jbc.RA118.001768
75. Watkins DW, Jenkins JMX, Grayson KJ, et al. Construction and in vivo assembly of a catalytically proficient and hyperthermostable de novo enzyme. *Nat Commun*. 2017;8(1):358. doi:10.1038/s41467-017-00541-4
76. Jenkins JMX, Noble CEM, Grayson KJ, Mulholland AJ, Anderson JLR. Substrate promiscuity of a *de novo* designed peroxidase. *J Inorg Biochem*. 2021;217:111370. doi:10.1016/j.jinorgbio.2021.111370
77. Hardy BJ, Martin Hermosilla A, Chinthapalli DK, Robinson CV, Anderson JLR, Curnow P. Cellular production of a de novo membrane cytochrome. *Proc Natl Acad Sci USA*. 2023;120(16):e2300137120. doi:10.1073/pnas.2300137120

78. Fry HC, Wood AR, Solomon LA. Supramolecular control of heme binding and electronic states in multi-heme peptide assemblies. *Org Biomol Chem*. 2017;15(32):6725-6730. doi:10.1039/C7OB01081H
79. Fry HC, Divan R, Liu Y. Designing 1D Multiheme peptide amphiphile assemblies reminiscent of natural systems. *Nanoscale*. 2022;14(28):10082-10090. doi:10.1039/D2NR00473A
80. Zozulia O, Korendovych IV. Semi-rationally designed short peptides self-assemble and bind hemin to promote cyclopropanation. *Angew Chem Int Ed*. 2020;59(21):8108-8112. doi:10.1002/anie.201916712
81. Luo W, Noguchi H, Chen C, et al. De novo designed peptides form a highly catalytic ordered nanoarchitecture on a graphite surface. *Nanoscale*. 2022;14(23):8326-8331. doi:10.1039/D2NR01507B
82. Dieckmann GR, McRorie DK, Tierney DL, et al. De novo design of mercury-binding two- and three-helical bundles. *J Am Chem Soc*. 1997;119(26):6195-6196. doi:10.1021/ja964351i
83. Matzapetakis M, Farrer BT, Weng T-C, Hemmingsen L, Penner-Hahn JE, Pecoraro VL. Comparison of the binding of cadmium (II), mercury (II), and arsenic (III) to the de novo designed peptides TRI L12C and TRI L16C. *J Am Chem Soc*. 2002;124(27):8042-8054. doi:10.1021/ja017520u
84. Matzapetakis M, Ghosh D, Weng T-C, Penner-Hahn JE, Pecoraro VL. Peptidic models for the binding of Pb(II), Bi(III) and Cd(II) to mononuclear thiolate binding sites. *JBIC J Biol Inorg Chem*. 2006;11(7):876-890. doi:10.1007/s00775-006-0140-7
85. Lee K-H, Matzapetakis M, Mitra S, Marsh ENG, Pecoraro VL. Control of metal coordination number in de novo designed peptides through subtle sequence modifications. *J Am Chem Soc*. 2004;126(30):9178-9179. doi:10.1021/ja048839s
86. Ruckthong L, Deb A, Hemmingsen L, Penner-Hahn JE, Pecoraro VL. Incorporation of second coordination sphere D-amino acids alters Cd(II) geometries in designed thiolate-rich proteins. *JBIC J Biol Inorg Chem*. 2018;23(1):123-135. doi:10.1007/s00775-017-1515-7
87. Lee K, Cabello C, Hemmingsen L, Marsh ENG, Pecoraro VL. Using nonnatural amino acids to control metal-coordination number in three-stranded coiled coils. *Angew Chem Int Ed*. 2006;45(18):2864-2868. doi:10.1002/anie.200504548
88. Ruckthong L, Zastrow ML, Stuckey JA, Pecoraro VL. A crystallographic examination of predisposition versus preorganization in de novo designed metalloproteins. *J Am Chem Soc*. 2016;138(36):11979-11988. doi:10.1021/jacs.6b07165
89. Touw DS, Nordman CE, Stuckey JA, Pecoraro VL. Identifying important structural characteristics of arsenic resistance proteins by using designed three-stranded coiled coils. *Proc Natl Acad Sci*. 2007;104(29):11969-11974. doi:10.1073/pnas.0701979104
90. Zastrow ML, Peacock AFA, Stuckey JA, Pecoraro VL. Hydrolytic catalysis and structural stabilization in a designed metalloprotein. *Nat Chem*. 2012;4(2):118-123. doi:10.1038/nchem.1201
91. Tegoni M, Yu F, Bersellini M, Penner-Hahn JE, Pecoraro VL. Designing a functional type 2 copper center that has nitrite reductase activity within α-helical coiled coils. *Proc Natl Acad Sci*. 2012;109(52):21234-21239. doi:10.1073/pnas.1212893110
92. Frost SC, McKenna R (Eds). *Carbonic anhydrase: mechanism, regulation, links to disease, and industrial applications*. Vol. 75. Springer Netherlands; 2014. doi:10.1007/978-94-007-7359-2
93. Angeli A, Carta F, Supuran CT. Carbonic anhydrases: versatile and useful biocatalysts in chemistry and biochemistry. *Catalysts*. 2020;10(9):1008. doi:10.3390/catal10091008
94. Supuran CT. Structure and function of carbonic anhydrases. *Biochem J*. 2016;473(14):2023-2032. doi:10.1042/BCJ20160115
95. Kim JK, Lee C, Lim SW, et al. Elucidating the role of metal ions in carbonic anhydrase catalysis. *Nat Commun*. 2020;11(1):4557. doi:10.1038/s41467-020-18425-5
96. Zastrow ML, Pecoraro VL. Designing hydrolytic zinc metalloenzymes. *Biochemistry*. 2014;53(6):957-978. doi:10.1021/bi4016617
97. Sprigings TG, Hall CD. A simple carbonic anhydrase model which achieves catalytic hydrolysis by the formation of an 'enzyme–substrate'-like complex. *J Chem Soc Perkin Trans 2*. 2001;(11):2063-2067. doi:10.1039/B107683N
98. Bazzicalupi C, Bencini A, Bianchi A, et al. Carboxy and phosphate esters cleavage with mono- and dinuclear zinc(II) macrocyclic complexes in aqueous solution. Crystal structure of $[Zn_2L_1(\mu\text{-}PP)_2(MeOH)_2](ClO_4)_2$ ($L_1$ = [30]aneN$_6$O$_4$, PP- = diphenyl phosphate). *Inorg Chem*. 1997;36(13):2784-2790. doi:10.1021/ic961521j
99. Bryson JW, Desjarlais JR, Handel TM, Degrado WF. From coiled coils to small globular proteins: design of a native-like three-helix bundle. *Protein Sci*. 1998;7(6):1404-1414. doi:10.1002/pro.5560070617
100. Cangelosi VM, Deb A, Penner-Hahn JE, Pecoraro VL. A De novo designed metalloenzyme for the hydration of $CO_2$. *Angew Chem Int Ed*. 2014;53(30):7900-7903. doi:10.1002/anie.201404925
101. Koebke KJ, Pecoraro VL. Development of de novo copper nitrite reductases: where we are and where we need to go. *ACS Catal*. 2018;8(9):8046-8057. doi:10.1021/acscatal.8b02153
102. Horrell S, Kekilli D, Strange RW, Hough MA. Recent structural insights into the function of copper nitrite reductases. *Metallomics*. 2017;9(11):1470-1482. doi:10.1039/c7mt00146k
103. Adman ET. Copper Protein Structures. In: Anfinsen CB, Edsall JT, Richards FM, Eisenberg DS, eds. *Advances in protein chemistry*. Vol.42, Metalloproteins: Structural Aspects. Academic Press; 1991:145-197. doi:10.1016/S0065-3233(08)60536-7
104. Liu J, Chakraborty S, Hosseinzadeh P, et al. Metalloproteins containing cytochrome, iron–sulfur, or copper redox centers. *Chem Rev*. 2014;114(8):4366-4469. doi:10.1021/cr400479b
105. Rubino JT, Franz KJ. Coordination chemistry of copper proteins: how nature handles a toxic cargo for essential function. *J Inorg Biochem*. 2012;107(1):129-143. doi:10.1016/j.jinorgbio.2011.11.024
106. Solomon EI, Baldwin MJ, Lowery MD. Electronic structures of active sites in copper proteins: contributions to reactivity. *Chem Rev*. 1992;92(4):521-542. doi:10.1021/cr00012a003
107. Rose SL, Baba S, Okumura H, et al. Single crystal spectroscopy and multiple structures from one crystal (MSOX) define catalysis in copper nitrite reductases. *Proc Natl Acad Sci USA*. 2022;119(30):e2205664119. doi:10.1073/pnas.2205664119
108. Koebke KJ, Yu F, Salerno E, et al. Modifying the steric properties in the second coordination sphere of designed peptides leads to enhancement of nitrite reductase activity. *Angew Chem Int Ed*. 2018;57(15):3954-3957. doi:10.1002/anie.201712757
109. Koebke KJ, Tebo AG, Manickas EC, Deb A, Penner-Hahn JE, Pecoraro VL. Nitrite reductase activity within an antiparallel de novo scaffold. *JBIC J Biol Inorg Chem*. 2021;26(7):855-862. doi:10.1007/s00775-021-01889-1
110. Pinter TBJ, Manickas EC, Tolbert AE, et al. Making or breaking metal-dependent catalytic activity: the role of stammers in designed three-stranded coiled coils. *Angew Chem Int Ed*. 2020;59(46):20445-20449. doi:10.1002/anie.202008356
111. Ghosh D, Pecoraro VL. Understanding metalloprotein folding using a de novo design strategy. *Inorg Chem*. 2004;43(25):7902-7915. doi:10.1021/ic048939z
112. Der BS, Edwards DR, Kuhlman B. Catalysis by a de novo zinc-mediated protein Interface: implications for natural enzyme evolution and rational enzyme engineering. *Biochemistry*. 2012;51(18):3933-3940. doi:10.1021/bi201881p
113. Studer S, Hansen DA, Pianowski ZL, et al. Evolution of a highly active and enantiospecific metalloenzyme from short peptides. *Science*. 2018;362(6420):1285-1288. doi:10.1126/science.aau3744
114. Basler S, Studer S, Zou Y, et al. Efficient Lewis acid catalysis of an abiological reaction in a de novo protein scaffold. *Nat Chem*. 2021;13(3):231-235. doi:10.1038/s41557-020-00628-4
115. Negi S, Imanishi M, Hamori M, et al. The past, present, and future of artificial zinc finger proteins: design strategies and chemical and biological applications. *JBIC J Biol Inorg Chem*. 2023;28(3):249-261. doi:10.1007/s00775-023-01991-6

116. Srivastava KR, Durani S. Design of a zinc-finger hydrolase with a synthetic Aββ protein. *PLoS ONE*. 2014;9(5):e96234. doi:10.1371/journal.pone.0096234
117. Patel K, Srivastava KR, Durani S. Zinc-finger hydrolase: computational selection of a linker and a sequence towards metal activation with a synthetic Aββ protein. *Bioorg Med Chem*. 2010;18(23):8270-8276. doi:10.1016/j.bmc.2010.10.003
118. Carvalho HF, Branco RJF, Leite FAS, Matzapetakis M, Roque ACA, Iranzo O. Hydrolytic zinc metallopeptides using a computational multi-state design approach. *Cat Sci Technol*. 2019;9(23):6723-6736. doi:10.1039/C9CY01364D
119. Lee M, Wang T, Makhlynets OV, et al. Zinc-binding structure of a catalytic amyloid from solid-state NMR. *Proc Natl Acad Sci*. 2017;114(24):6191-6196. doi:10.1073/pnas.1706179114
120. Rufo CM, Moroz YS, Moroz OV, et al. Short peptides self-assemble to produce catalytic amyloids. *Nat Chem*. 2014;6(4):303-309. doi:10.1038/nchem.1894
121. Marshall LR, Jayachandran M, Lengyel-Zhand Z, et al. Synergistic interactions are prevalent in catalytic amyloids. *ChemBioChem*. 2020;21(18):2611-2614. doi:10.1002/cbic.202000205
122. Lengyel-Zhand Z, Marshall LR, Jung M, et al. Covalent linkage and macrocylization preserve and enhance synergistic interactions in catalytic amyloids. *ChemBioChem*. 2021;22(3):585-591. doi:10.1002/cbic.202000645
123. Makhlynets OV, Gosavi PM, Korendovych IV. Short self-assembling peptides are able to bind to copper and activate oxygen. *Angew Chem Int Ed*. 2016;55(31):9017-9020. doi:10.1002/anie.201602480
124. Ishigami I, Sierra RG, Su Z, et al. Structural insights into functional properties of the oxidized form of cytochrome c oxidase. *Nat Commun*. 2023;14(1):5752. doi:10.1038/s41467-023-41533-x
125. Ipsen JØ, Hallas-Møller M, Brander S, Lo Leggio L, Johansen KS. Lytic polysaccharide monooxygenases and other histidine-brace copper proteins: structure, oxygen activation and biotechnological applications. *Biochem Soc Trans*. 2021;49(1):531-540. doi:10.1042/BST20201031
126. Baron AJ, Stevens C, Wilmot C, et al. Structure and mechanism of galactose oxidase. The free radical site. *J Biol Chem*. 1994;269(40):25095-25105. doi:10.1016/S0021-9258(17)31504-1
127. Johnson BJ, Yukl ET, Klema VJ, Klinman JP, Wilmot CM. Structural snapshots from the oxidative half-reaction of a copper amine oxidase: implications for $O_2$ activation. *J Biol Chem*. 2013;288(39):28409-28417. doi:10.1074/jbc.M113.501791
128. Mitra S, Prakash D, Rajabimoghadam K, et al. De novo design of a self-assembled artificial copper peptide that activates and reduces peroxide. *ACS Catal*. 2021;11(16):10267-10278. doi:10.1021/acscatal.1c02132
129. Prakash D, Mitra S, Murphy M, Chakraborty S. Oxidation and peroxygenation of C–H bonds by artificial Cu peptides (ArCuPs): improved catalysis via selective outer sphere modifications. *ACS Catal*. 2022;12(14):8341-8351. doi:10.1021/acscatal.2c01882
130. Lubitz W, Ogata H, Rüdiger O, Reijerse E. Hydrogenases. *Chem Rev*. 2014;114(8):4081-4148. doi:10.1021/cr4005814
131. Prasad P, Selvan D, Chakraborty S. Biosynthetic approaches towards the design of artificial hydrogen-evolution catalysts. *Chem A Eur J*. 2020;26(55):12494-12509. doi:10.1002/chem.202001338
132. Malayam Parambath S, Williams AE, Hunt LA, Selvan D, Hammer NI, Chakraborty S. A De novo-designed artificial metallopeptide hydrogenase: insights into photochemical processes and the role of protonated Cys. *ChemSusChem*. 2021;14(10):2237-2246. doi:10.1002/cssc.202100122
133. Prasad P, Hunt LA, Pall AE, et al. Photocatalytic hydrogen evolution by a de novo designed metalloprotein that undergoes Ni-mediated oligomerization shift. *Chem - Eur J*. 2023;29(14):e202202902. doi:10.1002/chem.202202902
134. Yoon JH, Kulesha AV, Lengyel-Zhand Z, et al. Uno Ferro, a de novo designed protein, binds transition metals with high affinity and stabilizes Semiquinone radical anion. *Chem - Eur J*. 2019;25(67):15252-15256. doi:10.1002/chem.201904020
135. Maiti BK, Almeida RM, Moura I, Moura JJG. Rubredoxins derivatives: simple sulphur-rich coordination metal sites and its relevance for biology and chemistry. *Coord Chem Rev*. 2017;352:379-397. doi:10.1016/j.ccr.2017.10.001
136. Pavone V, Gaeta G, Lombardi A, et al. Discovering protein secondary structures: classification and description of isolated α-turns. *Biopolymers*. 1996;38(6):705-721. doi:10.1002/(SICI)1097-0282(199606)38:6<705::AID-BIP3>3.0.CO;2-V
137. Nanda V, Rosenblatt MM, Osyczka A, et al. De novo design of a redox-active minimal rubredoxin mimic. *J Am Chem Soc*. 2005;127(16):5804-5805. doi:10.1021/ja050553f
138. Meyer J, Moulis J-M. Rubredoxin. In: *Handbook of Metalloproteins*. John Wiley & Sons, Ltd; 2006. doi:10.1002/0470028637.met135
139. Jacques A, Clémancey M, Blondin G, Fourmond V, Latour JM, Sénèque O. A cyclic peptide-based redox-active model of Rubredoxin. *Chem Commun*. 2013;49(28):2915-2917. doi:10.1039/C3CC40517F
140. Lombardi A, Marasco D, Maglio O, Di Costanzo L, Nastri F, Pavone V. Miniaturized metalloproteins: application to iron-sulfur proteins. *Proc Natl Acad Sci USA*. 2000;97(22):11922-11927. doi:10.1073/pnas.97.22.11922
141. Chino M, Di Costanzo LF, Leone L, et al. Designed rubredoxin miniature in a fully artificial electron chain triggered by visible light. *Nat Commun*. 2023;14(1):2368. doi:10.1038/s41467-023-37941-8
142. Pinto AF, Todorovic S, Hildebrandt P, et al. Desulforubrerythrin from Campylobacter jejuni, a novel multidomain protein. *JBIC J Biol Inorg Chem*. 2011;16(3):501-510. doi:10.1007/s00775-010-0749-4
143. La Gatta S, Leone L, Maglio O, et al. Unravelling the structure of the tetrahedral metal-binding site in METP3 through an experimental and computational approach. *Molecules*. 2021;26(17):5221. doi:10.3390/molecules26175221
144. Tebo AG, Pinter TBJ, García-Serres R, et al. Development of a rubredoxin-type center embedded in a *de dovo* -designed three-helix bundle. *Biochemistry*. 2018;57(16):2308-2316. doi:10.1021/acs.biochem.8b00091
145. Chakraborty S, Yudenfreund Kravitz J, Thulstrup PW, et al. Design of a three-helix bundle capable of binding heavy metals in a triscysteine environment. *Angew Chem Int Ed*. 2011;50(9):2049-2053. doi:10.1002/anie.201006413
146. Bragança PMS, Carepo MSP, Pauleta SR, et al. Incorporation of a molybdenum atom in a rubredoxin-type centre of a de novo-designed α3DIV-L21C three-helical bundle peptide. *J Inorg Biochem*. 2023;240:112096. doi:10.1016/j.jinorgbio.2022.112096
147. Maiti BK, Maia LB, Silveira CM, et al. Incorporation of molybdenum in rubredoxin: models for mononuclear molybdenum enzymes. *JBIC J Biol Inorg Chem*. 2015;20(5):821-829. doi:10.1007/s00775-015-1268-0
148. Dennison C. Investigating the structure and function of cupredoxins. *Coord Chem Rev*. 2005;249(24):3025-3054. doi:10.1016/j.ccr.2005.04.021
149. Shiga D, Nakane D, Inomata T, et al. Creation of a type 1 blue copper site within a de novo coiled-coil protein scaffold. *J Am Chem Soc*. 2010;132(51):18191-18198. doi:10.1021/ja106263y
150. Koebke KJ, Alfaro VS, Pinter TBJ, et al. Traversing the red–green–blue color spectrum in rationally designed cupredoxins. *J Am Chem Soc*. 2020;142(36):15282-15294. doi:10.1021/jacs.0c04757
151. Li H, Webb SP, Ivanic J, Jensen JH. Determinants of the relative reduction potentials of Type-1 copper sites in proteins. *J Am Chem Soc*. 2004;126(25):8010-8019. doi:10.1021/ja049345y
152. Marks J, Pozdnyakova I, Guidry J, Wittung-Stafshede P. Methionine-121 coordination determines metal specificity in unfolded Pseudomonas aeruginosa azurin. *JBIC J Biol Inorg Chem*. 2004;9(3):281-288. doi:10.1007/s00775-004-0523-6

153. Shiga D, Hamano Y, Kamei M, et al. Tuning the geometries of a de novo blue copper protein by axial interactions. *JBIC J Biol Inorg Chem*. 2012;17(7):1025-1031. doi:10.1007/s00775-012-0916-x
154. Basumallick L, Szilagyi RK, Zhao Y, Shapleigh JP, Scholes CP, Solomon EI. Spectroscopic studies of the Met182Thr mutant of nitrite reductase: role of the axial ligand in the geometric and electronic structure of blue and green copper sites. *J Am Chem Soc*. 2003;125(48):14784-14792. doi:10.1021/ja037232t
155. Plegaria JS, Duca M, Tard C, et al. *De novo* design and characterization of copper metallopeptides inspired by native cupredoxins. *Inorg Chem*. 2015;54(19):9470-9482. doi:10.1021/acs.inorgchem.5b01330
156. Plegaria JS, Dzul SP, Zuiderweg ERP, Stemmler TL, Pecoraro VL. Apoprotein structure and metal binding characterization of a *de novo* designed peptide, $\alpha_3$D IV, that sequesters toxic heavy metals. *Biochemistry*. 2015;54(18):2858-2873. doi:10.1021/acs.biochem.5b00064
157. Plegaria JS, Herrero C, Quaranta A, Pecoraro VL. Electron transfer activity of a de novo designed copper center in a three-helix bundle fold. *Biochim Biophys Acta BBA - Bioenerg*. 2016;1857(5):522-530. doi:10.1016/j.bbabio.2015.09.007
158. Koebke KJ, Ruckthong L, Meagher JL, et al. Clarifying the copper coordination environment in a *de novo* designed red copper protein. *Inorg Chem*. 2018;57(19):12291-12302. doi:10.1021/acs.inorgchem.8b01989
159. Jung S-M, Lee J, Song WJ. Design of artificial metalloenzymes with multiple inorganic elements: the more the merrier. *J Inorg Biochem*. 2021;223:111552. doi:10.1016/j.jinorgbio.2021.111552
160. Sazinsky MH, Lippard SJ. Correlating structure with function in bacterial multicomponent monooxygenases and related diiron proteins. *Acc Chem Res*. 2006;39(8):558-566. doi:10.1021/ar030204v
161. Osborne CD, Haritos VS. Beneath the surface: evolution of methane activity in the bacterial multicomponent monooxygenases. *Mol Phylogenet Evol*. 2019;139:106527. doi:10.1016/j.ympev.2019.106527
162. Sazinsky MH, Lippard SJ. Methane monooxygenase: functionalizing methane at iron and copper. In: Kroneck PMH, Sosa Torres ME, eds. *Sustaining life on planet earth: Metalloenzymes mastering dioxygen and other chewy gases, metal ions in life sciences*. Springer International Publishing; 2015:205-256. doi:10.1007/978-3-319-12415-5_6
163. Rosenzweig AC, Nordlund P, Takahara PM, Frederick CA, Lippard SJ. Geometry of the soluble methane monooxygenase catalytic diiron center in two oxidation states. *Chem Biol*. 1995;2(6):409-418. doi:10.1016/1074-5521(95)90222-8
164. Tinberg CE, Lippard SJ. Dioxygen activation in soluble methane monooxygenase. *Acc Chem Res*. 2011;44(4):280-288. doi:10.1021/ar1001473
165. Sakai Y, Yurimoto H, Shima S. Methane monooxygenases; physiology, biochemistry and structure. *Catal Sci Technol*. 2023;13(22):6342-6354. doi:10.1039/D3CY00737E
166. Sudarev VV, Dolotova SM, Bukhalovich SM, et al. Ferritin self-assembly, structure, function, and biotechnological applications. *Int J Biol Macromol*. 2023;224:319-343. doi:10.1016/j.ijbiomac.2022.10.126
167. Greene BL, Kang G, Cui C, et al. Ribonucleotide reductases: structure, chemistry, and metabolism suggest new therapeutic targets. *Annu Rev Biochem*. 2020;89(1):45-75. doi:10.1146/annurev-biochem-013118-111843
168. Summa CM, Lombardi A, Lewis M, DeGrado WF. Tertiary templates for the design of diiron proteins. *Curr Opin Struct Biol*. 1999;9(4):500-508. doi:10.1016/S0959-440X(99)80071-2
169. Lombardi A, Pirro F, Maglio O, Chino M, DeGrado WF. De novo design of four-helix bundle metalloproteins: one scaffold, diverse reactivities. *Acc Chem Res*. 2019;52(5):1148-1159. doi:10.1021/acs.accounts.8b00674
170. Chino M, Maglio O, Nastri F, Pavone V, DeGrado WF, Lombardi A. Artificial diiron enzymes with a de novo designed four-helix bundle structure. *Eur J Inorg Chem*. 2015;2015(21):3371-3390. doi:10.1002/ejic.201500470
171. Lombardi A, Summa CM, Geremia S, Randaccio L, Pavone V, DeGrado WF. Retrostructural analysis of metalloproteins: application to the design of a minimal model for diiron proteins. *Proc Natl Acad Sci USA*. 2000;97(12):6298-6305. doi:10.1073/pnas.97.12.6298
172. Faiella M, Andreozzi C, de Rosales RTM, et al. An artificial di-iron oxo-protein with phenol oxidase activity. *Nat Chem Biol*. 2009;5(12):882-884. doi:10.1038/nchembio.257
173. Reig AJ, Pires MM, Snyder RA, et al. Alteration of the oxygen-dependent reactivity of de novo Due Ferri proteins. *Nat Chem*. 2012;4(11):900-906. doi:10.1038/nchem.1454
174. Chino M, Leone L, Maglio O, et al. A de novo heterodimeric Due Ferri protein minimizes the release of reactive intermediates in dioxygen-dependent oxidation. *Angew Chem Int Ed*. 2017;56(49):15580-15583. doi:10.1002/anie.201707637
175. Pirro F, Schmidt N, Lincoff J, et al. Allosteric cooperation in a de novo-designed two-domain protein. *Proc Natl Acad Sci*. 2020;117(52):33246-33253. doi:10.1073/pnas.2017062117
176. Maglio O, Nastri F, Pavone V, Lombardi A, DeGrado WF. Preorganization of molecular binding sites in designed Diiron proteins. *Proc Natl Acad Sci USA*. 2003;100(7):3772-3777. doi:10.1073/pnas.0730771100
177. Di Costanzo L, Wade H, Geremia S, et al. Toward the de novo design of a catalytically active helix bundle: a substrate-accessible carboxylate-bridged dinuclear metal center. *J Am Chem Soc*. 2001;123(51):12749-12757. doi:10.1021/ja010506x
178. Maglio O, Nastri F, Calhoun JR, et al. Artificial di-iron proteins: solution characterization of four helix bundles containing two distinct types of inter-helical loops. *JBIC J Biol Inorg Chem*. 2005;10(5):539-549. doi:10.1007/s00775-005-0002-8
179. Marsh ENG, DeGrado WF. Noncovalent self-assembly of a heterotetrameric diiron protein. *Proc Natl Acad Sci USA*. 2002;99(8):5150-5154. doi:10.1073/pnas.052023199
180. Kaplan J, DeGrado WF. De novo design of catalytic proteins. *Proc Natl Acad Sci USA*. 2004;101(32):11566-11570. doi:10.1073/pnas.0404387101
181. Martin T, de Rosales R, Faiella M, Farquhar E, et al. Spectroscopic and metal-binding properties of DF3: an artificial protein able to accommodate different metal ions. *JBIC. J Biol Inorg Chem*. 2010;15(5):717-728. doi:10.1007/s00775-010-0639-9
182. Berthold DA, Stenmark P. Membrane-bound diiron carboxylate proteins. *Annu Rev Plant Biol*. 2003;54(1):497-517. doi:10.1146/annurev.arplant.54.031902.134915
183. Calhoun JR, Kono H, Lahr S, Wang W, DeGrado WF, Saven JG. Computational design and characterization of a monomeric helical dinuclear metalloprotein. *J Mol Biol*. 2003;334(5):1101-1115. doi:10.1016/j.jmb.2003.10.004
184. Bell CBI, Calhoun JR, Bobyr E, et al. Spectroscopic definition of the biferrous and biferric sites in de novo designed four-helix bundle DFsc peptides: implications for $O_2$ reactivity of binuclear non-heme iron enzymes. *Biochemistry*. 2009;48(1):59-73. doi:10.1021/bi8016087
185. Snyder RA, Butch SE, Reig AJ, DeGrado WF, Solomon EI. Molecular-level insight into the differential oxidase and oxygenase reactivities of de novo Due Ferri proteins. *J Am Chem Soc*. 2015;137(29):9302-9314. doi:10.1021/jacs.5b03524
186. Snyder RA, Betzu J, Butch SE, Reig AJ, DeGrado WF, Solomon EI. Systematic perturbations of binuclear non-Heme iron sites: structure and dioxygen reactivity of de novo Due Ferri proteins. *Biochemistry*. 2015;54(30):4637-4651. doi:10.1021/acs.biochem.5b00324
187. Ulas G, Lemmin T, Wu Y, Gassner GT, DeGrado WF. Designed metalloprotein stabilizes a semiquinone radical. *Nat Chem*. 2016;8(4):354-359. doi:10.1038/nchem.2453
188. Kulesha A, Yoon JH, Chester C, D'Souza A, Costeas C, Makhlynets OV. Contributions of primary coordination ligands and importance of outer sphere interactions in UFsc, a de novo designed protein

with high affinity for metal ions. *J Inorg Biochem*. 2020;212:111224. doi:10.1016/j.jinorgbio.2020.111224

189. Paredes A, Loh BM, Peduzzi OM, Reig AJ, Buettner KM. DNA cleavage by a de novo designed protein–titanium complex. *Inorg Chem*. 2020;59(16):11248-11252. doi:10.1021/acs.inorgchem.0c01707
190. Sazinsky MH, Bard J, Di Donato A, Lippard SJ. Crystal structure of the toluene/o-xylene monooxygenase hydroxylase from Pseudomonas stutzeri OX1: insight into the substrate specificity, substrate channeling, and active site tuning of multicomponent monooxygenases. *J Biol Chem*. 2004;279(29):30600-30610. doi:10.1074/jbc.M400710200
191. Chino M, Leone L, Maglio O, Lombardi A. Chapter Twenty-One - Designing covalently linked heterodimeric four-helix bundles. In: Pecoraro VL, ed. *Methods in enzymology*. Vol.580, Peptide, Protein and Enzyme Design. Academic Press; 2016:471-499. doi:10.1016/bs.mie.2016.05.036
192. Polizzi NF, Wu Y, Lemmin T, et al. De novo design of a hyperstable non-natural protein–ligand complex with sub-Å accuracy. *Nat Chem*. 2017;9(12):1157-1164. doi:10.1038/nchem.2846
193. Ogihara NL, Ghirlanda G, Bryson JW, Gingery M, DeGrado WF, Eisenberg D. Design of three-dimensional domain-swapped dimers and fibrous oligomers. *Proc Natl Acad Sci USA*. 2001;98(4):1404-1409. doi:10.1073/pnas.98.4.1404
194. Wittkamp F, Senger M, Stripp ST, Apfel U-P. [FeFe]-hydrogenases: recent developments and future perspectives. *Chem Commun*. 2018;54(47):5934-5942. doi:10.1039/C8CC01275J
195. Morra S. Fantastic [FeFe]-hydrogenases and where to find them. *Front Microbiol*. 2022;13:853626. doi:10.3389/fmicb.2022.853626
196. Rodríguez-Maciá P, Galle LM, Bjornsson R, et al. Caught in the Hinact: crystal structure and spectroscopy reveal a sulfur bound to the active site of an O2-stable state of [FeFe] hydrogenase. *Angew Chem Int Ed*. 2020;59(38):16786-16794. doi:10.1002/anie.202005208
197. Simmons TR, Berggren G, Bacchi M, Fontecave M, Artero V. Mimicking hydrogenases: from biomimetics to artificial enzymes. *Coord Chem Rev*. 2014;270–271:127-150. doi:10.1016/j.ccr.2013.12.018
198. Leone L, Sgueglia G, La Gatta S, et al. Enzymatic and bioinspired systems for hydrogen production. *Int J Mol Sci*. 2023;24(10):8605. doi:10.3390/ijms24108605
199. Jones AK, Lichtenstein BR, Dutta A, Gordon G, Dutton PL. Synthetic hydrogenases: incorporation of an iron carbonyl thiolate into a designed peptide. *J Am Chem Soc*. 2007;129(48):14844-14845. doi:10.1021/ja075116a
200. Apfel U-P, Rudolph M, Apfel C, et al. Reaction of $Fe_3(CO)_{12}$ with octreotide—chemical, electrochemical and biological investigations. *Dalton Trans*. 2010;39(12):3065-3071. doi:10.1039/B921299J
201. Roy S, Nguyen T-AD, Gan L, Jones AK. Biomimetic peptide-based models of [FeFe]-hydrogenases: utilization of phosphine-containing peptides. *Dalton Trans*. 2015;44(33):14865-14876. doi:10.1039/C5DT01796C
202. Sano Y, Onoda A, Hayashi T. A hydrogenase model system based on the sequence of cytochrome c: photochemical hydrogen evolution in aqueous media. *Chem Commun*. 2011;47(29):8229-8231. doi:10.1039/C1CC11157D
203. Shafaat HS, Rüdiger O, Ogata H, Lubitz W. [NiFe] hydrogenases: a common active site for hydrogen metabolism under diverse conditions. *Biochim Biophys Acta BBA - Bioenerg*. 2013;1827(8):986-1002. doi:10.1016/j.bbabio.2013.01.015
204. Ogata H, Lubitz W, Higuchi Y. Structure and function of [NiFe] hydrogenases. *J Biochem (Tokyo)*. 2016;160(5):251-258. doi:10.1093/jb/mvw048
205. Tang H, Hall MB. Biomimetics of [NiFe]-hydrogenase: nickel- or iron-centered proton reduction catalysis? *J Am Chem Soc*. 2017;139(49):18065-18070. doi:10.1021/jacs.7b10425
206. Dutta A, Hamilton GA, Hartnett HE, Jones AK. Construction of heterometallic clusters in a small peptide scaffold as [NiFe]-hydrogenase models: development of a synthetic methodology. *Inorg Chem*. 2012;51(18):9580-9588. doi:10.1021/ic2026818
207. Timm J, Pike DH, Mancini JA, et al. Design of a minimal di-nickel hydrogenase peptide. *Sci Adv*. 2023;9(10):eabq1990. doi:10.1126/sciadv.abq1990
208. Stevenson MJ, Marguet SC, Schneider CR, Shafaat HS. Light-driven hydrogen evolution by nickel-substituted rubredoxin. *ChemSusChem*. 2017;10(22):4424-4429. doi:10.1002/cssc.201701627
209. Selvan D, Prasad P, Farquhar ER, et al. Redesign of a copper storage protein into an artificial hydrogenase. *ACS Catal*. 2019;9(7):5847-5859. doi:10.1021/acscatal.9b00360
210. Shiga D, Funahashi Y, Masuda H, et al. Creation of a binuclear purple copper site within a de novo coiled-coil protein. *Biochemistry*. 2012;51(40):7901-7907. doi:10.1021/bi3007884
211. Pirro F, La Gatta S, Arrigoni F, et al. A De novo-designed type 3 copper protein tunes catechol substrate recognition and reactivity. *Angew Chem Int Ed*. 2023;62(1):e202211552. doi:10.1002/anie.202211552
212. Kroneck PMH. Walking the seven lines: binuclear copper a in cytochrome c oxidase and nitrous oxide reductase. *JBIC J Biol Inorg Chem*. 2018;23(1):27-39. doi:10.1007/s00775-017-1510-z
213. Carreira C, Pauleta SR, Moura I. The catalytic cycle of nitrous oxide reductase — the enzyme that catalyzes the last step of denitrification. *J Inorg Biochem*. 2017;177:423-434. doi:10.1016/j.jinorgbio.2017.09.007
214. Guo J, Fisher OS. Orchestrating copper binding: structure and variations on the cupredoxin fold. *JBIC J Biol Inorg Chem*. 2022;27(6):529-540. doi:10.1007/s00775-022-01955-2
215. Solomon EI, Chen P, Metz M, Lee S-K, Palmer AE. Oxygen binding, activation, and reduction to water by copper proteins. *Angew Chem Int Ed*. 2001;40(24):4570-4590. doi:10.1002/1521-3773(20011217)40:24<4570::AID-ANIE4570>3.0.CO;2-4
216. Yoon J, Fujii S, Solomon EI. Geometric and electronic structure differences between the type 3 copper sites of the multicopper oxidases and hemocyanin/tyrosinase. *Proc Natl Acad Sci USA*. 2009;106(16):6585-6590. doi:10.1073/pnas.0902127106
217. Kampatsikas I, Rompel A. Similar but still different: which amino acid residues are responsible for varying activities in type-III copper enzymes? *ChemBioChem*. 2021;22(7):1161-1175. doi:10.1002/cbic.202000647
218. Nakamura K, Go N. Function and molecular evolution of multicopper blue proteins. *Cell Mol Life Sci CMLS*. 2005;62(18):2050-2066. doi:10.1007/s00018-004-5076-x
219. Gräff M, Buchholz PCF, Le Roes-Hill M, Pleiss J. Multicopper oxidases: modular structure, sequence space, and evolutionary relationships. *Proteins Struct Funct Bioinform*. 2020;88(10):1329-1339. doi:10.1002/prot.25952
220. Krężel A, Maret W. The bioinorganic chemistry of mammalian metallothioneins. *Chem Rev*. 2021;121(23):14594-14648. doi:10.1021/acs.chemrev.1c00371
221. Kharenko OA, Kennedy DC, Demeler B, Maroney MJ, Ogawa MY. Cu(I) luminescence from the tetranuclear $Cu_4S_4$ cofactor of a synthetic 4-helix bundle. *J Am Chem Soc*. 2005;127(21):7678-7679. doi:10.1021/ja042757m
222. Xie F, Sutherland DEK, Stillman MJ, Ogawa MY. Cu(I) binding properties of a designed metalloprotein. *J Inorg Biochem*. 2010;104(3):261-267. doi:10.1016/j.jinorgbio.2009.12.005
223. Zaytsev DV, Morozov VA, Fan J, et al. Metal-binding properties and structural characterization of a self-assembled coiled coil: formation of a polynuclear Cd–thiolate cluster. *J Inorg Biochem*. 2013;119:1-9. doi:10.1016/j.jinorgbio.2012.10.010
224. Beinert H. Iron-sulfur proteins: ancient structures, still full of surprises. *JBIC J Biol Inorg Chem*. 2000;5(1):2-15. doi:10.1007/s007750050002

225. Imlay JA. Iron-sulphur clusters and the problem with oxygen. *Mol Microbiol*. 2006;59(4):1073-1082. doi:10.1111/j.1365-2958.2006.05028.x
226. Lill R. From the discovery to molecular understanding of cellular iron-sulfur protein biogenesis. *Biol Chem*. 2020;401(6–7):855-876. doi:10.1515/hsz-2020-0117
227. Rouault TA. Mammalian iron–sulphur proteins: novel insights into biogenesis and function. *Nat Rev Mol Cell Biol*. 2015;16(1):45-55. doi:10.1038/nrm3909
228. Balk J, Pilon M. Ancient and essential: the assembly of iron–sulfur clusters in plants. *Trends Plant Sci*. 2011;16(4):218-226. doi:10.1016/j.tplants.2010.12.006
229. Sweeney WV, Rabinowitz JC. Proteins containing 4Fe-4S clusters: an overview. *Annu Rev Biochem*. 1980;49(1):139-161. doi:10.1146/annurev.bi.49.070180.001035
230. Goris T, Wait AF, Saggu M, et al. A unique iron-sulfur cluster is crucial for oxygen tolerance of a [NiFe]-hydrogenase. *Nat Chem Biol*. 2011;7(5):310-318. doi:10.1038/nchembio.555
231. Berto P, Di Valentin M, Cendron L, et al. The [4Fe–4S]-cluster coordination of [FeFe]-hydrogenase maturation protein HydF as revealed by EPR and HYSCORE spectroscopies. *Biochim Biophys Acta BBA - Bioenerg*. 2012;1817(12):2149-2157. doi:10.1016/j.bbabio.2012.09.004
232. Morales R, Charon M, Kachalova G, et al. A redox-dependent interaction between two electron-transfer partners involved in photosynthesis. *EMBO Rep*. 2000;1(3):271-276. doi:10.1093/embo-reports/kvd057
233. Gibney BR, Mulholland SE, Rabanal F, Dutton PL. Ferredoxin and ferredoxin–heme maquettes. *Proc Natl Acad Sci USA*. 1996;93(26):15041-15046. doi:10.1073/pnas.93.26.15041
234. Mulholland SE, Gibney BR, Rabanal F, Dutton PL. Characterization of the fundamental protein ligand requirements of $[4Fe\text{-}4S]^{2+/+}$ clusters with sixteen amino acid maquettes. *J Am Chem Soc*. 1998;120(40):10296-10302. doi:10.1021/ja981279a
235. Mulholland SE, Gibney BR, Rabanal F, Dutton PL. Determination of nonligand amino acids critical to $[4Fe\text{-}4S]^{2+/+}$ assembly in ferredoxin maquettes. *Biochemistry*. 1999;38(32):10442-10448. doi:10.1021/bi9908742
236. Kennedy ML, Gibney BR. Proton coupling to $[4Fe\text{-}4S]^{2+/+}$ and $[4Fe\text{-}4Se]^{2+/+}$ oxidation and reduction in a designed protein. *J Am Chem Soc*. 2002;124(24):6826-6827. doi:10.1021/ja0171613
237. Bombana A, Shanmugam M, Collison D, et al. Application of a synthetic ferredoxin-inspired [4Fe4S]-peptide maquette as the redox partner for an [FeFe]-hydrogenase. *ChemBioChem*. 2023;24(18):e202300250. doi:10.1002/cbic.202300250
238. Grzyb J, Xu F, Weiner L, et al. De novo design of a non-natural fold for an iron–sulfur protein: alpha-helical coiled-coil with a four-iron four-sulfur cluster binding site in its central core. *Biochim Biophys Acta BBA - Bioenerg*. 2010;1797(3):406-413. doi:10.1016/j.bbabio.2009.12.012
239. Han GW, Yang X-L, McMullan D, et al. Structure of a tryptophanyl-tRNA synthetase containing an iron–sulfur cluster. *Acta Crystallogr Sect F Struct Biol Cryst Commun*. 2010;66(10):1326-1334. doi:10.1107/S1744309110037619
240. Grzyb J, Xu F, Nanda V, et al. Empirical and computational design of iron-sulfur cluster proteins. *Biochim Biophys Acta BBA - Bioenerg*. 2012;1817(8):1256-1262. doi:10.1016/j.bbabio.2012.02.001
241. Roy A, Sarrou I, Vaughn MD, Astashkin AV, Ghirlanda G. De novo design of an artificial bis[4Fe-4S] binding protein. *Biochemistry*. 2013;52(43):7586-7594. doi:10.1021/bi401199s
242. Roy A, Sommer DJ, Schmitz RA, et al. A De novo designed 2[4Fe-4S] ferredoxin mimic mediates electron transfer. *J Am Chem Soc*. 2014;136(49):17343-17349. doi:10.1021/ja510621e
243. Kim JD, Pike DH, Tyryshkin AM, et al. Minimal heterochiral de novo designed 4Fe–4S binding peptide capable of robust electron transfer. *J Am Chem Soc*. 2018;140(36):11210-11213. doi:10.1021/jacs.8b07553
244. Smith ET, Feinberg BA. Redox properties of several bacterial ferredoxins using square wave voltammetry. *J Biol Chem*. 1990;265(24):14371-14376. doi:10.1016/S0021-9258(18)77311-0
245. Anderson JLR, Armstrong CT, Kodali G, et al. Constructing a man-made c-type cytochrome maquette in vivo: electron transfer, oxygen transport and conversion to a photoactive light harvesting maquette. *Chem Sci*. 2013;5(2):507-514. doi:10.1039/C3SC52019F
246. Jagilinki BP, Ilic S, Trncik C, et al. In vivo biogenesis of a de novo designed iron–sulfur protein. *ACS Synth Biol*. 2020;9(12):3400-3407. doi:10.1021/acssynbio.0c00514
247. Lubitz W, Chrysina M, Cox N. Water oxidation in photosystem II. *Photosynth Res*. 2019;142(1):105-125. doi:10.1007/s11120-019-00648-3
248. Zhang S-Q, Chino M, Liu L, et al. De novo design of tetranuclear transition metal clusters stabilized by hydrogen-bonded networks in helical bundles. *J Am Chem Soc*. 2018;140(4):1294-1304. doi:10.1021/jacs.7b08261
249. Shen J-R. The structure of photosystem II and the mechanism of water oxidation in photosynthesis. *Annu Rev Plant Biol*. 2015;66(1):23-48. doi:10.1146/annurev-arplant-050312-120129
250. Zabret J, Bohn S, Schuller SK, et al. Structural insights into photosystem II assembly. *Nat Plants*. 2021;7(4):524-538. doi:10.1038/s41477-021-00895-0
251. Bhowmick A, Hussein R, Bogacz I, et al. Structural evidence for intermediates during $O_2$ formation in photosystem II. *Nature*. 2023;617(7961):629-636. doi:10.1038/s41586-023-06038-z
252. Kamada S, Nakajima Y, Shen J-R. Structural insights into the action mechanisms of artificial electron acceptors in photosystem II. *J Biol Chem*. 2023;299(7):104839. doi:10.1016/j.jbc.2023.104839
253. Paul S, Neese F, Pantazis DA. Structural models of the biological oxygen-evolving complex: achievements, insights, and challenges for biomimicry. *Green Chem*. 2017;19(10):2309-2325. doi:10.1039/C7GC00425G
254. Chino M, Zhang S-Q, Pirro F, et al. Spectroscopic and metal binding properties of a de novo metalloprotein binding a tetrazinc cluster. *Biopolymers*. 2018;109(10):e23339. doi:10.1002/bip.23229
255. Olson TL, Espiritu E, Edwardraja S, et al. Design of dinuclear manganese cofactors for bacterial reaction centers. *Biochim Biophys Acta BBA - Bioenerg*. 2016;1857(5):539-547. doi:10.1016/j.bbabio.2015.09.003
256. Wade H, Stayrook SE, DeGrado WF. The structure of a designed diiron (III) protein: implications for cofactor stabilization and catalysis. *Angew Chem Int Ed*. 2006;45(30):4951-4954. doi:10.1002/anie.200600042
257. Olson TL, Espiritu E, Edwardraja S, et al. Biochemical and spectroscopic characterization of dinuclear Mn-sites in artificial four-helix bundle proteins. *Biochim Biophys Acta BBA - Bioenerg*. 2017;1858(12):945-954. doi:10.1016/j.bbabio.2017.08.013
258. Chino M, Leone L, Zambrano G, et al. Oxidation catalysis by iron and manganese porphyrins within enzyme-like cages. *Biopolymers*. 2018;109(10):e23107. doi:10.1002/bip.23107
259. Baglia RA, Zaragoza JPT, Goldberg DP. Biomimetic reactivity of oxygen-derived manganese and iron porphyrinoid complexes. *Chem Rev*. 2017;117(21):13320-13352. doi:10.1021/acs.chemrev.7b00180
260. Huang X, Groves JT. Oxygen activation and radical transformations in heme proteins and metalloporphyrins. *Chem Rev*. 2018;118(5):2491-2553. doi:10.1021/acs.chemrev.7b00373
261. Arad E, Jelinek R. Catalytic amyloids. *Trends Chem*. 2022;4(10):907-917. doi:10.1016/j.trechm.2022.07.001
262. Marshall LR, Korendovych IV. Catalytic amyloids: is misfolding folding? *Curr Opin Chem Biol*. 2021;64:145-153. doi:10.1016/j.cbpa.2021.06.010

## AUTHOR BIOGRAPHIES

**Linda Leone** is a research fellow at the University of Naples Federico II, where she obtained her PhD in Chemical Sciences in 2020. In 2019, she spent a period at the University of Bristol as a visiting PhD student. Linda works in the field of bioinorganic chemistry, focusing on the development of artificial metalloenzymes and their applications in chemical synthesis, renewable energy generation, and biomass valorization. Her research interests also include the synthesis and characterization of antimicrobial peptides and the construction of functional nanomaterials.

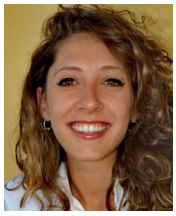

**Maria De Fenza** received her MS and PhD in Chemical Sciences from the University of Naples Federico II in 2015 and 2018, respectively. She then joined the research group of Prof. Angela Lombardi since 2019, where she is currently a research fellow. Throughout her career, Maria has undertaken several research periods abroad, including at the Rega Institute for Medical Research in Leuven, Oxford University as a visiting PhD student, and at Karolinska Institutet in Stockholm as a visiting researcher. Her research interests primarily focus on developing small molecules for therapeutic applications and investigating artificial protein models for biocatalysis.

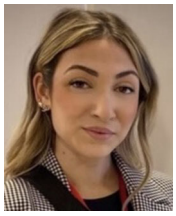

**Alessandra Esposito** is a PhD student in Chemical Sciences at the University of Naples Federico II. She earned her MS in Chemical Sciences in October 2021. In 2023, Alessandra spent a period as a visiting PhD student at the University of Cambridge. Her research focuses on generation of peptide-based functional nanomaterials crafting artificial heme-enzymes with amyloid fibrils.

**Ornella Maglio** received her PhD in Chemical Sciences from the University of Naples Federico II, in 1998. She was a visiting fellow at the National Institute of Medical Research in London, and currently, Ornella is a research associate professor at the Institute of Biostructures and Bioimaging of the CNR in Naples. Her research interests are in the field of de novo designed metallopeptides, artificial metalloenzymes, and bioactive peptides, covering the synthesis and their structural characterization, mainly by NMR.

**Flavia Nastri** is associate professor of General and Inorganic Chemistry at the University of Naples Federico II, where she received the PhD in Chemical Sciences in 1996. In 1994, she was visiting fellow at the Universitè Renè Descartes, Paris. Her research activity is focused on Bioinorganic Chemistry, dealing with the design, synthesis, and structural characterization of artificial molecules able to reproduce the active site of natural metalloproteins and metalloenzymes. Research activities also deals with the immobilization of artificial metalloenzymes and bioactive peptides on different supports for applications in nanotechnology.

**Angela Lombardi** received her PhD in Chemical Sciences in 1990 from the University of Naples Federico II, working in the area of transition metal chemistry and peptide synthesis. In the same year, she was tenured as research associate at the Department of Chemistry, where she is currently a professor of Inorganic and Bioinorganic Chemistry. Angela spent numerous sabbatical periods in the United Statesd: Sshe was visiting scientist at DuPont Merck Pharmaceutical Company, Wilmington (1995-1996), at the University of Pennsylvania (1997), and at the University of California, San Francisco (2013). Her research interests include the de novo design of peptide-based metalloprotein models, and their application in catalysis, energy production, construction of functional nanomaterials and biosensors. Angela's research interests also include bioactive peptides, such as antimicrobial peptides and amyloids, to exploit in biotechnological applications.

**How to cite this article:** Leone L, De Fenza M, Esposito A, Maglio O, Nastri F, Lombardi A. Peptides and metal ions: A successful marriage for developing artificial metalloproteins. *J Pept Sci*. 2024;30(10):e3606. doi:10.1002/psc.3606